Phenotypic variations in the growth of lettuce seedlings as affected by the surrounding microenvironment and management factors

January 2022

Eri Hayashi

Graduate School of Horticulture

CHIBA UNIVERSITY

（千葉大学審査学位論文）

Phenotypic variations in the growth of lettuce seedlings as affected by the surrounding microenvironment and management factors

January 2022

Eri Hayashi

Graduate School of Horticulture

CHIBA UNIVERSITY

Table of Contents

Chapter 1. Introduction

1.1 Overview of the global situation of plant factories with artificial lighting----------4

1.2 Current challenge of PFALs----------5

1.3 Plant phenotyping as a potential application to commercial PFALs ----------7

Chapter 2. Phenotypic analysis of germination time of individual seed as affected by microenvironment and management factors for plant cohort research in PFALs

2.1 Introduction----------11

2.2 Materials and methods----------14

2.3 Results----------21

2.4 Discussion----------27

2.5 Conclusions----------29

Chapter 3. Variations in the growth of cotyledons and initial true leaves as affected by photosynthetic photon flux density at individual seedlings and nutrients

3.1 Introduction----------31

3.2 Materials and methods----------33

3.3 Results----------41

3.4 Discussion----------51

3.5 Conclusions----------54

Chapter 4. Variations in the seedling growth as affected by the time-course changes in photosynthetic photon flux density

4.1 Introduction----------55

4.2 Materials and methods----------56

4.3 Results----------61

4.4 Discussion----------64

4.5 Conclusions----------66

Chapter 5. Conclusions ----------67

References----------69

Chapter 1. Introduction

1.1 Overview of the global situation of plant factories with artificial lighting

A plant factory with artificial lighting (PFAL) is a closed plant production system with an almost airtight and well-insulated structure, that allows for increased resource utilization efficiency. The environment is precisely controlled to produce high quantities of high-quality plants year-round, entirely independent of outdoor conditions [1–11]. Occasionally, a difference in terminology is observed among countries, organizations, and individuals, such as PFAL, vertical farm/farming, and indoor agriculture [12]. The term PFAL, as used in this dissertation, refers to "an environmentally controlled plant production system with artificial lighting in a thermally insulated and almost airtight facility."

PFALs are attracting attention worldwide as a novel plant production system that contributes to the solution of significant global challenges, including food, environment, energy, resources, human health. Despite individual differences in the background or motivation for operating a PFAL, countless dynamic opportunities and possibilities have emerged in recent years. In fact, particularly since 2015, an increasing number of people or organizations with diverse backgrounds have become involved in the PFAL business, system development, and research [12]. PFALs are increasingly being developed and operated in Japan and many other countries, including China, Singapore, other countries in Asia and Europe, the United States [12], North America, and the Middle East.

From a historical viewpoint, research and development of PFALs in Japan began in the mid-1970s [13–15]. Since initially being established in Japan in the early 1980s, commercial PFALs with high-pressure sodium (HPS) lamps and multi-layered cultivation systems with fluorescent lamps (FLs) have become apparent in Japan [13].

While its numbers gradually increased each year in the 2000s, 2009 marked the start of the third PFAL movement in Japan [16]. In addition to government-funded projects, mainly by the Ministry of Economy, Trade, and Industry (METI) and the Ministry of Agriculture, Forestry, and Fisheries (MAFF), a large number of Japanese companies with various backgrounds started to enter the PFAL industry as growers and

system manufacturers [16]. In terms of commercialization, after the initial growth in the 1980s and the 1990s, approximately 200 commercial PFALs have been operating in Japan since 2009 [17].

Furthermore, particularly since 2017, the PFAL industry in Japan has been shifting into the fourth movement, which includes scalability and introduction of new technologies such as automation and information technology (IT) among others [12]. Figure 1-1 shows the interior view of the cultivation room of the 808 Factory, Shinnippou, located in Shizuoka Prefecture, Japan, which produces 20,000 lettuce heads every day, using light-emitting diodes (LEDs) [12].

Figure 1-1. Interior view of the cultivation room of the 808 Factory, Shinnippou. (Photo courtesy of Shinnippou)

1.2 Current challenge of PFALs

Considering the potential of PFALs in contributing concurrently to the solution of significant global challenges, including food, environment, energy, resources, and public health, there is further room for improvement, in the technical and economic aspects [18]. The theoretical benefits of the PFAL can be achieved only when the system

is properly engineered, constructed, and operated [18–20]. In practice, a variety of PFAL challenges remain, including high initial investment, optimal cultivation systems, environmental controls, plant growth, and socioeconomic impact [10,20]. These challenges can be overcome by improving PFAL productivity [20].

The productivity of a PFAL can be described by the resource type used, including materials, energy, time, and space invested, along with monetary terms [20]. Table 1-1 shows the estimated productivity of major commercial PFALs in Japan. It covers the volume of salable products, and most of the major commercial PFALs harvest and pack leafy lettuce head, not precut lettuce, in Japan. Therefore, the uniformity of plant growth of each head is essential to improve productivity, maintain plant morphology, and ensure the absence of physiological disorders, such as tip burn.

Table 1-1. Estimated resource productivity of commercial PFALs in Japan [20].

Resources applied	**Range of resource productivity**	**Range of monetary productivity (kg/USD)**	**Range of production cost (USD/kg)**
Electric energy	0.11–0.14 kg kWh^{-1}	0.645–0.755	1.09–1.28
Labor hours	7.7–10.0 kg h^{-1}	0.591–0.770	1.18–1.63
Cultivation area (per day)	0.25–0.33 kg m^{-2} d^{-1}	0.482–0.645	1.28–1.72
Other resources	-	0.609–0.827	1.00–1.36
Total	-	0.166–0.219	4.55–5.99

American dollar. In 2019, one USD and one Euro were 110 JPY and 130 JPY, respectively. Note that wages ($/hour) are around two times higher in the USA and some European countries than in Japan as of 2021.

However, despite the controlled environment in PFALs, variations in individual plant have been found, especially around harvesting [6,11,21,22]. These variations adversely affect plant productivity during PFAL operations [6,11,21,22]. Although the plant growth on the cultivation tray seemed to be uniform at first glance, relatively large

variations in the fresh weight per plant were found [21]. Similar variations in plant height, morphology, and concentrations of secondary metabolites per plant were observed [21].

Uniformity of plant growth by reducing two-dimensional (2D) variations in plant growth or traits (i.e., phenotypes) can contribute to improving productivity in PFALs [21]. Variations in the plant traits of individual plants are mainly attributable to three factors: environment, genotype (species and cultivar), and management (human and machine intervention, seed treatments) [6,11,21]. The 2D variations in plant traits over a cultivation tray are partially ascribed to 2D variations in the surrounding microenvironment of individual plants, including photosynthetic photon flux density (PPFD) and air current speed over and within the plant canopy or individuals in the tray, among other factors [21]. Previous studies have revealed the time-course changes in the PPFD distribution over the cultivation tray, depending on the stages of plant growth, as well as the difference in the PPFD distribution between a plant canopy and the cultivation tray without plants [23–26].

Seed germination and the initial seedling stage are among the most critical stages of plant growth [6,21,27–31]. The ecophysiological status of individual plants affects the subsequent plant growth processes [6,21,27–31]. Variations in the timing of germination and growth of individual seedlings substantially affect the uniformity of plant growth, and consequently, plant productivity in PFALs. For instance, the difference in germination timing results in a more significant growth difference, even a couple of days after sowing [21]. Therefore, it is essential to reveal the variations in individual germination time and initial growth of each seedling and to elucidate how they are affected by the surrounding microenvironments and management factors.

1.3 Plant phenotyping and its potential application in commercial PFALs

Plant phenotyping plays an integral role in understanding how the microenvironment surrounding individual plants and their management, including seed treatments, affects variations in the phenotype of individual plants [6,11,21,32–34]. Plant phenotyping is a set of methodologies and protocols used to study plant performance, growth, architecture, and composition at different organization scales, from organs to

canopies (Table 1-2) [5,6,11,21,32–34]. It reveals plant trait dynamics or the time course of plant phenotypes in a non-destructive and non-invasive manner [6,11,21,32–34]. A phenotyping system is a tool for the nondestructive or noninvasive measurement of the time course of plant phenotypes. Among the units to be developed using advanced technologies for the advancement of PFALs, the phenotyping system is among the most important for improving productivity of plant production in PFALs [21].

Table 1-2. Definitions of the term "phenome" and related terms used in this paper [5].

Phenome (P): A whole set of observable traits (or characteristics) at the cell, tissue, organ, individual, and population levels.	**Genome (G):** 1) One haploid set of chromosomes with genes. 2) Broadly, the genetic material of an organism.
Phenotype: 1) A subset of the phenome. 2) A set of observable traits determined by genetic and environmental (and human/machine intervention) influences.	**Genotype:** 1) A subset of the genome. 2) A group of organisms with the same genetic constitution.
Phenotyping: Process of determining the phenotype.	**Genotyping:** Process of determining the genotype.
Phenomics: A research field involving phenomes, phenotypes, phenotyping, and their application.	**Genomics:** A research field involving genomes, genotypes, genotyping and their application.

Over the past years, the focus of phenotyping studies has been on developing high-throughput, accurate, and rapid phenotyping systems, in addition to image processing algorithms in the field [32,35]. In phenomics, phenotypic traits have been measured in multiple dimensions, including 2D measurement to obtain the projected leaf area using digital image processing [36,37]. Phenotyping has the potential to be applied in commercial PFALs [38].

Image-based PFAL studies have been conducted over the years. The projected leaf area (measured using 2D camera images captured from above the plant canopy or

seedling trays) of the plant canopy using camera images in PFALs was also attempted [11,22,39–47]. Furthermore, some studies have used red-green-blue (RGB) camera images to quantify the projected leaf area and estimate the light energy consumption per plant [45].

However, most previous studies on PFALs have been limited to the mean values of plant populations, there by lacking a focus on the individual plants. Moreover, the average values of environmental data, such as PPFD, have been estimated, rather than the values of data associated with the microenvironment of individual plants. In most previous studies, the frequency of image capture used to estimate the projected leaf area has been limited to a few times per day or even a week. Therefore, to elucidate the variations in plant phenotypes in the microenvironment of individual plants and how these variations are affected by the microenvironment, it is critical to measure plant phenotypes based on time-series data.

This dissertation reports the exploration of variation in the plant phenotype or growth of individual plants to analyze how phenotypic variations are affected by the surrounding microenvironment and management factors, using time series 2D images. A modular plant phenotype measurement system for germination and seedling production was developed that focused on practicality and scalability in commercial PFALs, achieving a low cost with small cameras and sensors, and a cultivation method similar to commercial PFALs. Experiments on the germination and initial seedling stages of romaine lettuce (*Lactuca sativa* L. var. longifolia), which strongly affects plant productivity, were conducted as part of the plant life cycle research.

First, phenotypic analysis of the effect of the microenvironment and management factors in PFALs on the germination time of individual seeds has been discussed based on time series image data. Then, in a serial study, experiments on the initial stage of seedlings, as one of the critical initial stages of plant growth, were conducted. Specifically, variations in the growth of cotyledons and initial true leaves, affected by PPFD at individual seedlings and nutrients, were studied to elucidate how the surrounding microenvironment of individual plants affects the variations in individual seedlings. Furthermore, the effects of PPFD in the cultivation space, in particular the

time-course changes in PPFD in response to seedling growth, were examined to determine the effects of the time-course microenvironment on seedling growth.

Chapter 2. Phenotypic analysis of germination time of individual seeds affected by microenvironment and management factors for cohort research in PFALs

2.1. Introduction

Understanding how microenvironment and management factors affect variations in germination time of individual seeds is an important step towards robust and consistent agricultural productions. Variations in the traits (i.e., phenotypes) of individual plants are attributable to mainly three factors: environment, genotype (specific to species and cultivar), and management (human and/or machine intervention), including seed treatments. Plant phenotyping plays a crucial role in understanding these interactions [11,21,32]. Plant phenotyping is a set of methodologies and protocols used to study plant growth, performance, architecture, and composition at different scales of organization, from organs to canopies, and it reveals the plant trait dynamics in a non-invasive and non-destructive manner [11,21,32–34]. These measured traits may display macro- and micro-environmental variations [48]. Over the past years, the focus has been put on developing high-throughput accurate and rapid phenotyping systems together with image processing algorithms, which possesses potential to be adapted also for the study under controlled environmental conditions [32,35,38].

Plant factory with artificial lighting (PFAL) is a closed plant production system, with an almost airtight and well-insulated structure, which allows increased resource utilization efficiency under a precisely controlled environment to produce high quantities of high-quality plants year-round, completely independently of outdoor conditions [1–11]. However, despite the highly controlled environment in PFAL, the variations in plant individuals have been found specifically at the time of harvesting, urging the development of a new phenotypic analysis platform [11,21,22].

Seed germination is one of the most important initial stages of plant growth, and the ecophysiological status of germinated seeds has an impact on the subsequent plant growth process [21,27]. Germination is generally defined as emergence of the radicle through the surrounding structure after water uptake by the seed [49,50]. Germination

time from sowing to outbreak of the radicle from seed coat (germination time hereafter) and its uniformity of seeds are essential for plant growth, as they consequently affect the productivity of plant production. Plant seeds have complex phenotypes that are difficult to quantitatively assess [51]. Therefore, measurement of seed germination is one of the important initial stages of plant phenotyping.

Measurement of seed germination has gained much attention from plant growers, seed scientists, and other plant biologists. Seeds from different individual plants, populations, seed lots and treatments all influence germination percentages, speed, and uniformity [27]. Germination time provides valuable information about the favorability of germination conditions [50]. In order to achieve uniform harvests, it is important to identify the causes of the variations in seed germination time and eliminate those factors that contribute to the variability [21]. The time course curves produced in seed germination tests provide considerable information about germination time and its uniformity of seeds [49].

However, measurement of seed germination has been limited to the germination percentage over a population of seeds that have completed germination at a given time, but not the germination time of an individual seed [49]. Indeed, the outputs of various measurement methods of seed germination that have been adopted for many years have been a mean or median of germination time or percentage of specific seed lots. The past studies have indicated the limitations of these methods [27,49,52,53]. To achieve accurate quantification of germination, there have been studies including high-throughput automatic scoring and evaluation of germination [54,55]. However, how microenvironment and management factors affect germination time of individual seeds and subsequent plant growth has not been investigated in detail. In order to elucidate the individual phenotype variations, it is essential to measure germination time of individual seeds and to analyze how microenvironment and management factors affect individual germination time and subsequent plant growth.

In this study, a plant phenotype measurement system was developed to assess germination time (*GT*) of individual seeds of romaine lettuce (*Lactuca sativa* L. var. longifolia) in seed trays each with 300 seeds, using time series data on two-dimensional

(2D) camera images, and to analyze each germination time as affected by its surrounding microenvironment (volumetric water percent of the substrate in each tray, individual seed surface temperature and air temperature) and management factors (coated and uncoated seeds) of individual seeds. Using this system, plant cohort research was conducted in this study as an initial stage of the whole plant growth process. The modular system was designed with an emphasis on practicality and scalability in commercial plant production in PFALs. This system achieves low cost with small cameras and sensors, along with cultivation method similar to the one in commercial PFALs. Experiments on germination were conducted to demonstrate the performance of the system and its applicability for a whole plant growth process in a PFAL for large-scale commercial production and/or breeding. This present study is part of and will contribute to a broader plant cohort research project.

In the plant cohort research, the life cycle phenome history of individual plants can be measured continuously and noninvasively, and analyzed from seed sowing to harvesting by using phenotyping units, along with the time course data on environment, management, and resource inputs/outputs in PFAL [4–6,11,21,47]. Plant cohort refers to a relatively large group of plant individuals with a statistical factor (such as cultivar, planting density, and cultivation system) in common with the plants in a PFAL for commercial plant production and/or breeding [4–6,11,21,47]. For the plant cohort research, the time series data sets in the data warehouse (DWH) can be used, which leads to identification of an optimal set points of environmental factors for maximizing multi-objective function, and concurrently improve plant productivity and breed new cultivars in PFAL [4–6,11,21,47].

Through this study, germination time of individual seeds were obtained from time series 2D camera images by using the developed plant phenotype measurement system as an initial stage of the plant cohort research in PFALs. Furthermore, the phenotyping platform revealed the effects of microenvironment and management factors on germination time of individual seeds.

2.2. Materials and Methods

2.2.1. Description of the System

A germination container box (GCB) equipped with phenotyping and microenvironmental sensing units was designed and developed (Figure 2-1). GCB consists of five major units and parts: temperature control (A–C), phenotyping (D–G), sensors (H), cultivation (I–K), and an exterior box frame (L) (Figure 2-1a). The original GCB (WR-60CHL-S; Keibunsha Seisakusho, Hiroshima, Japan) was composed of an air conditioner, air outlet of air conditioner, and electric heater, which were built in an exterior box with frame (A, B, C, and L, respectively; Figure 2-1a, b).

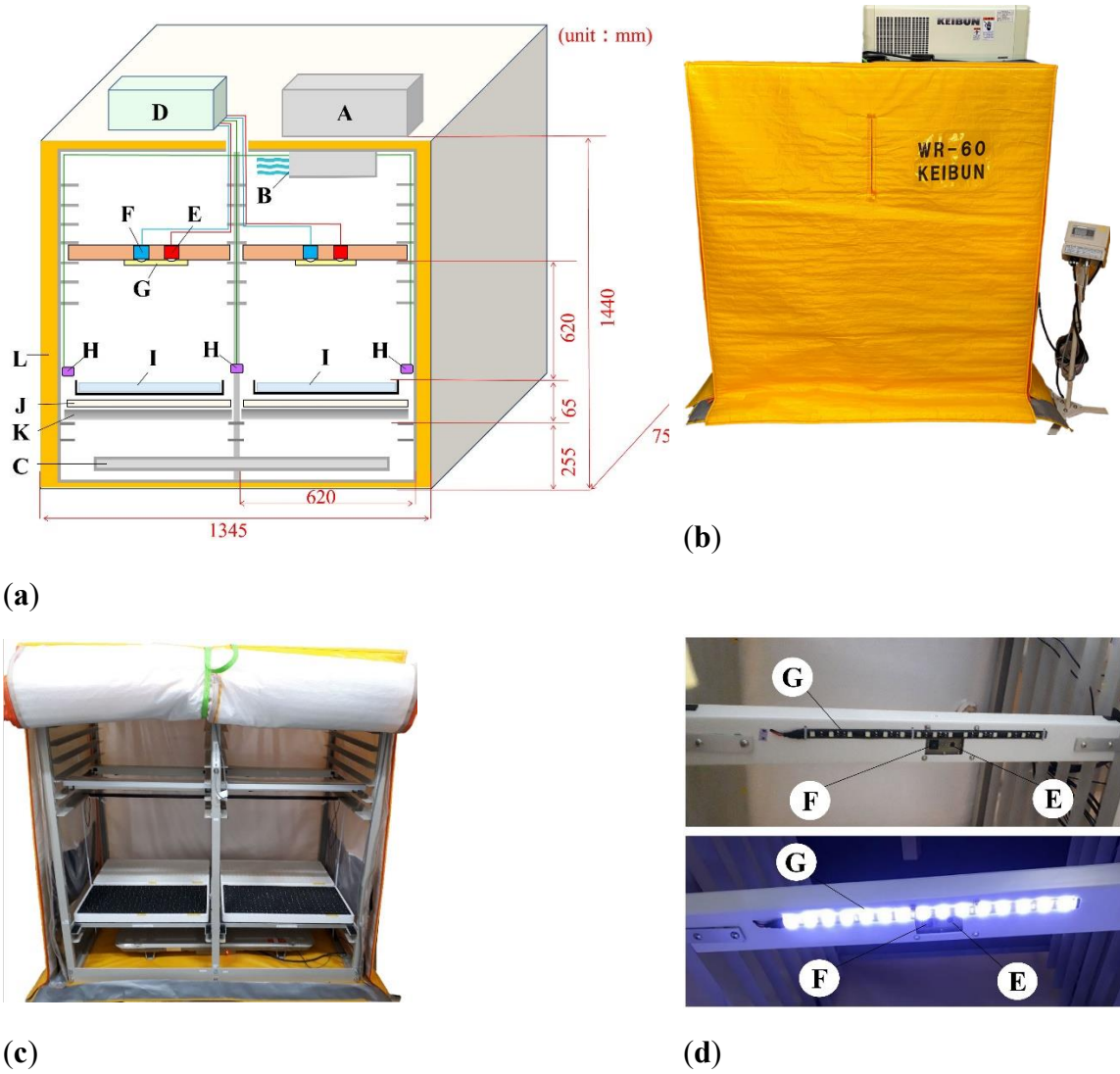

Figure 2-1. Germination container box (GCB) equipped with phenotyping and

microenvironmental sensing units. (a) Schematic diagram. 1) Temperature control unit: Air conditioner (A), Air outlet of air conditioner (B), Electric heater (C). 2) Phenotyping unit: Control board (×4) (D), Red-green-blue (RGB) camera (×4) (E), Thermal camera (×4) (F), White light emitting diode (LED) for flash (×4) (G). 3) Air temperature/relative humidity sensor (×4) (H). 4) Cultivation unit: Seed tray with substrate (seed tray) (×4) (I), Acrylic plate (J), Reinforcement bar (K). 5) Exterior box with frame (L); (b) Exterior of GCB; (c) Inside view of GCB; (d) Phenotyping unit with the flash off (upper image) and on (lower image).

Phenotyping and microenvironmental sensing and cultivation units were additionally installed to GCB; newly installed items include a control board (Raspberry Pi 3 Model B; Raspberry Pi Foundation, Cambridge, United Kingdom) (×4), red-green-blue (RGB) camera (Raspberry Pi Pi NoIR Camera Module V2; Raspberry Pi Foundation, Cambridge, United Kingdom) (×4), thermal camera (FLIR Lepton 3.5; FLIR Systems, Inc., Wilsonville, OR, USA) (×4), white light emitting diode (LED) for flash of RGB camera (15 white LED tape, 300 mm) (SOF-15W-30-3SMD; Tokulumi Co., Ltd., Kwai Chung, Hong Kong) (×4), air temperature/relative humidity sensor (AM2302; Guangzhou Aosong Electronics Co., Ltd., Guangzhou, China) (×4), seed tray with substrate (seed tray) (605 × 300 × 42 mm) (×4), acrylic plate (thickness: 3 mm), and reinforcement bar (thickness: 20 mm) (D, E, F, G, H, I, J, K; Figure 2-1a).

The phenotyping units, sets of RGB camera, thermal camera (160 × 120 pixel, with temperature measurement function), and LED were installed 620 mm above the surface of each seed tray (Figure 2-1c, d). As emphasizing the design principle for the phenotyping unit, cost-effectiveness and compactness were given priority for the selection of the cameras, with a vision to ultimately apply to commercial production in PFALs and breeding. Air temperature/relative humidity sensors were setup in the upper right/left of the cultivation trays. The cultivation unit contains space for four seed trays, designed to maintain consistency of each tray's location. Each substrate in the seed tray consists of 300 (= 25 × 12) foamed urethane cubes, each with a hole of 11.5 mm in diameter and 6 mm in depth. All seeds in each tray are numbered in accordance with the

position in the seed tray (P_i (i = 1 ~ 300)) (Figure 2-2). By using the air conditioner and electric heater built in the GCB, air temperature inside the GCB can be controlled within the range of 10 to 40 °C.

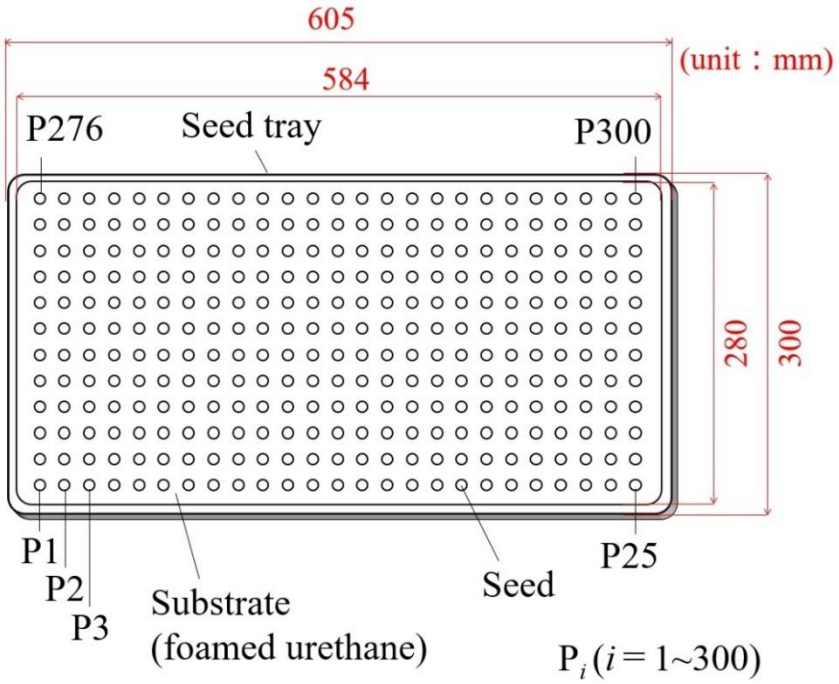

Figure 2-2. Plane view of seed tray with substrate consisting of 300 (= 25 × 12) foamed urethane cubes. All seeds in each tray are numbered in accordance with the position in the seed tray with plant seed number (P_i (i = 1 ~ 300)).

2.2.2. Phenotyping and Microenvironmental Sensing Units

For unification and analysis of time series data, a DWH was built [56] and further modified to improve operability. Each RGB camera, thermal camera, LED, and air temperature/relative humidity sensor (phenotyping and microenvironmental sensing unit) is connected to each control board and designed to be activated at specified time intervals (the shortest possible period of every one minute). All data obtained from phenotyping and microenvironmental sensing units are automatically sent to the DWH through the control boards.

To derive *GT* of individual seeds, the RGB camera was used to acquire time series 2D image data. The thermal camera was applied to obtain time series data of seed

surface temperature of individual seeds (*SST*). Prior to installing thermal cameras, calibration was performed using thermocouples. With the thermal camera, 19,200 pixels/surface temperatures of substrate per image are acquired. The system was programmed to extract *SST* (300 pixels per image/seed tray) automatically from the original thermal image. All *SST* data are assigned with consecutive seed numbers in the seed tray (P_i (i = 1~300)) (Figure 2-2).

2.2.3. Germination Time (GT) Acquired from RGB Image

GT of individual seeds were acquired from time series RGB images. Figure 2-3 shows the process of deriving *GT* from RGB images. Representative images with 0.5 h intervals are shown. The time series RGB images of seed trays were continuously obtained from the RGB camera at set intervals and then sent automatically to the DWH (Figure 2-3). One RGB image covers one seed tray that contains 300 seeds on a foamed urethan substrate (Figure 2-3). Each RGB image of seed tray is processed to be divided into 300 images of individual seeds. Then, these time series RGB images of each individual seed are re-sequenced in a chronological order (Figure 2-3).

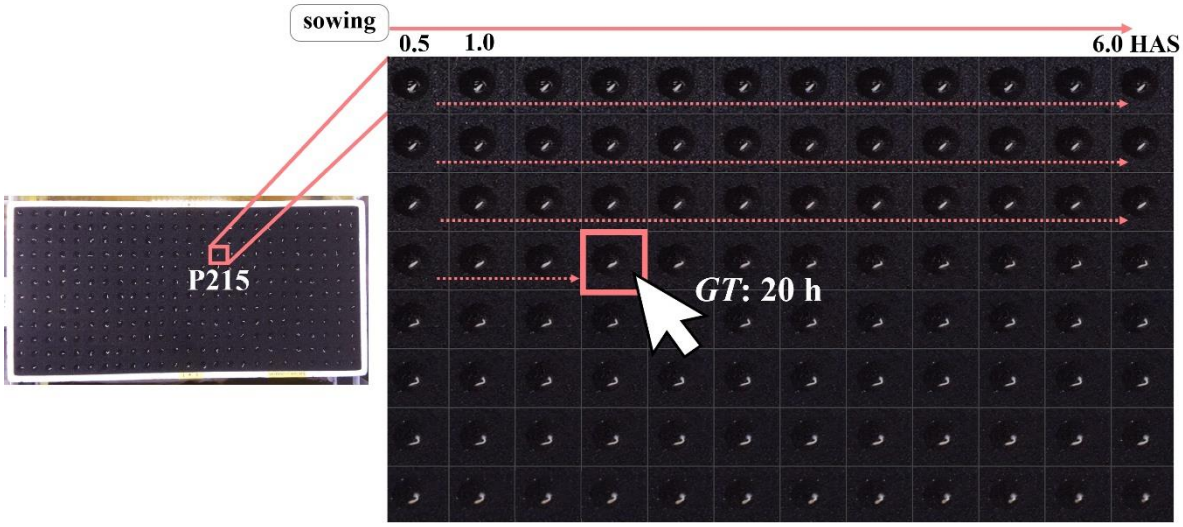

Figure 2-3. Process of acquiring germination time (*GT*) from time series red-green-blue (RGB) image data. Time series RGB images of seed trays were obtained from the RGB camera at set intervals and then sent automatically to the data warehouse (DWH) (left image). Each RGB image covers one seed tray with 300 seeds on a foamed urethan

substrate (left image). An example of marked seed number P215 is shown (left image). After each RGB image of seed tray is segmented into 300 images of individual seeds, time series of individual seed images are re-sequenced in a chronological order to determine *GT* by selecting the germinated seed (right image). Time course RGB data of seed P215 every 0.5 h (HAS: hours after sowing) with *GT* of 20 h is shown (right image).

To determine *GT*, the RGB image of a germinated seed was selected among the time course images of each seed (Figure 2-3). Binary judgement was made to all the RGB images to identify the presence (T) or absence (F) of germination, i.e., annotation. The decision criteria for the presence of germination were set as when approximately 1-mm-long root/radicle, extending from the outer seed coat or cracked coating, was observed. In addition to determining germination by RGB images, ground truth measurements from all actual seeds at 48 h after sowing (HAS), hours of imbibition/water absorption, were conducted to confirm or correct the original binary classification/annotation. The *GT* and binary classification/annotation data together with RGB image data were output to CSV files as data sets along with environment and management data.

2.2.4. Experimental Design

2.2.4.1. Data Acquisition

To demonstrate the performance of GCB with phenotyping and microenvironmental sensing units, experiments were conducted from seed sowing to 48 HAS (germination stage). For this experiment, the actuation time of the RGB camera, air temperature/relative humidity sensor and thermal camera were set at every 0.5 h, 0.17 h (10 min), and 48 h, respectively.

During the single germination stage, 96 RGB images (0.5 h × 48 h) per seed tray were obtained by each RGB camera. Twenty-eight thousand and eight hundred data sets with RGB images (300 seeds/seed tray × 96 RGB images), together with annotation data, *GT* of 300 seeds, and microenvironment and management data can be obtained from the single seed tray from one germination experiment. If four seed trays were used at once in GCB, 115,200 data sets (28,800 × 4 seed trays) can be obtained from a single experiment.

2.2.4.2. Variables and Symbols

List of symbols and variable names are described in Table 2-1. Besides *GT* and *SST*, average *GT* per 300 seeds in a seed tray ($\overline{GT}$), and average *SST* per 300 seeds in a seed tray 48 HAS ($\overline{SST}$) were calculated, respectively. Volumetric percentage of nutrient solution in seed tray (*VPNS*) was quantified, but not for each substrate for individual seeds in this study. Setpoint air temperature of GCB (*SAT*), air temperature inside the GCB (*AT*) and average *AT* at 48 HAS ($\overline{AT}$) were also collected. The germination percentage (*GP*) was calculated by the number of germinated seeds per 300 seeds in a seed tray 48 HAS. Furthermore, hourly germination rate (speed of germination) (*GR*) and average *GR* per 300 seeds in a seed tray 48 HAS ($\overline{GR} = GP/\overline{GT}$) were determined. For the data analysis of experimental results, software R, a language and environment for statistical computing and graphics, was used [57].

Table 2-1. List of symbols, variable names with descriptions and units.

Symbol	Variable name/Description	Unit
AT	Air temperature inside the germination container box (GCB)	°C
$\overline{AT}$	Average *AT* at 48 h after sowing (HAS)	
C	Coated seed	-
GP	Germination percentage per 300 seeds 48 HAS	%
GR	Hourly germination rate of individual seed (inverse of *GT*)	h^{-1}
$\overline{GR}$	Average *GR* per 300 seeds (*GP* divided by $\overline{GT}$)	% h^{-1}
GT	Germination time course (from seed sowing to outbreak of the radicle from seed coat) of individual seed	h
$\overline{GT}$	Average *GT* per 300 seeds	
SST	Seed surface temperature of individual seed	°C
$\overline{SST}$	Average *SST* per 300 seeds 48 HAS	
SAT	Setpoint air temperature of GCB	°C
U	Uncoated seed	-
VPNS	Volumetric percentage of nutrient solution in seed tray	%

2.2.4.3. Plant Material and Culture Conditions

To analyze *GT* as effected by its surrounding microenvironment and management factors, experiments on seed germination were carried out with a focus on altering air temperature (*SAT)* and volumetric water/nutrient solution percent in seed tray (*VPNS*), considering the two major elements for germination to occur: temperature and water [49,50]. Thus, as shown in Table 2-2, two kinds of experiments, altering either 1) *SAT* or 2) *VPNS* during the germination stage, were conducted:

1) *SAT* of 12 °C, 16 °C, 20 °C, 24 °C, 28 °C, 32 °C, 36 °C, and 40 °C, whereas *VPNS* was fixed at 86%, with management factors of uncoated seed (U) and coated seed (C), i.e., 16 conditions, and 2) *VPNS* of 77%, 82% and 86% as *SAT* was fixed at 20 °C [58] for both U and C, i.e., 6 conditions.

Table 2-2. Experimental design (see Table 2-1 for abbreviations).

	Treatments	Measured	Calculated
1)	*SAT*: 12 °C, 16 °C, 20 °C, 24 °C, 28 °C, 32 °C, 36 °C, 40 °C *VPNS*: 86% Seed type: U and C	*GT*, $\overline{GT}$ *SST*, $\overline{SST}$ *AT*, $\overline{AT}$ *GP*	*GR*, $\overline{GR}$ *CVt* (*St*/$\overline{GT}$) *CVt* (*St*/$\overline{SST}$)
2)	*SAT*: 20 °C *VPNS*: 77%, 82%, 86% Seed type: U and C		

As for management factors, two types of seeds (U and C) of romaine lettuce (*Lactuca sativa* L. var. longifolia, Lomaria, TLE487, offered by Takii & Co., Kyoto, Japan) were used. Substrates with color of black, made of flexible polyurethane foam (MIRAI Co., Ltd., Kashiwa, Japan, 584 × 280 × 28 mm, 300 wells, 12 mm in diameter × 6 mm deep), were used in the seed trays. For this study, black substrate, instead of white substrate, was chosen to facilitate an accurate detection of *GT* from RGB images.

For nutrient solution, Chiba University's lettuce formula [59] was used, with nutrient solution temperature, pH and electrical conductivity of 20 °C, 6.5 and 1.9 mS

cm^{-1}, respectively. In addition to automated data acquisition with phenotyping and microenvironmental sensing units and other environmental data, management data, such as culturist, time required for sowing, and identified numbers of germinated seeds from RGB images, were collected, along with seed type (U and C). The experiments were conducted under identical conditions: substrates were soaked in the set amount of nutrient solution and the same GCB was used.

Except when the flashes for RGB camera were on (10 s/time for photographing), inside the GCB was kept dark during the experiment: the photosynthetic photon flux density (PPFD) at the position of the seed tray was 0.03 to 0.05 μmol m^{-2} s^{-1}. The GCB was placed inside the environmentally controllable cultivation room of PFAL, located at Kashiwanoha Campus of Chiba University, with air temperature, relative humidity and CO_2 concentrations inside the cultivation room of 20 °C, 80~100% and 1500 μmol mol^{-1}, respectively.

2.3. Results

A plant phenotype measurement system was developed to assess *GT* of romaine lettuce (*L. sativa* L. var. longifolia) in seed trays each with 300 seeds, using time series data on 2D camera images, and to analyze each *GT* as affected by its surrounding microenvironment (*SST*, *VPNS*, and air temperature) and management (U and C) factors of individual seeds for plant cohort research. Experiments on germination were conducted to demonstrate the performance of the system and its applicability for a whole plant growth process in a PFAL for large-scale commercial production and/or breeding.

GT of individual seeds were acquired from time series RGB images (Figure 2-4). Figure 3 shows the process of deriving *GT* from RGB images. Representative images with 0.5 h intervals are shown. The time series RGB images of seed trays were continuously obtained from the RGB camera at set intervals and then sent automatically to the DWH (Figure 2-3). One RGB image covered one seed tray that contained 300 seeds on a foamed urethan substrate (Figure 2-3). Each RGB image of seed tray was processed to be divided into 300 images of individual seeds. Then, these time series RGB images of each individual seed were re-sequenced in a chronological order (Figure 2-3).

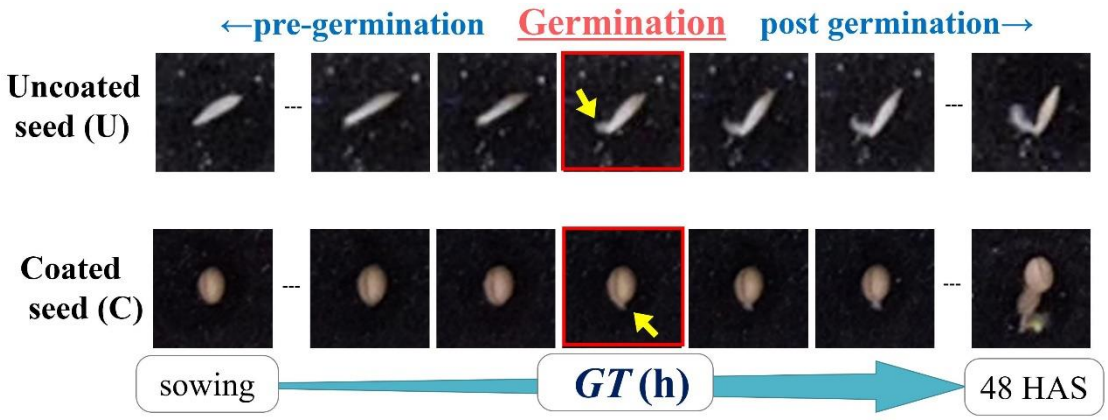

Figure 2-4. Germination time (*GT*) acquired from time series red-green-blue (RGB) images, obtained continuously from sowing until 48 h after sowing (HAS).

To determine *GT*, the RGB image of a germinated seed was selected among the time course images of each seed (Figure 2-3). Binary judgement was made to all the RGB images to identify the presence (T) or absence (F) of germination, i.e., annotation. The decision criteria for the presence of germination were set as when approximately 1-mm-long root/radicle, extending from the outer seed coat or cracked coating, was observed. In addition to determining germination by RGB images, ground truth measurements from all actual seeds at 48 HAS were conducted to confirm or correct the original binary classification/annotation. The *GT* and binary classification/annotation data together with RGB image data were output to CSV files as data sets along with environment and management data.

In addition to deriving *GT* of individual seeds from time series RGB camera, the thermal camera was applied to obtain time series data of seed surface temperature of individual seeds (*SST*). With the thermal camera, 19,200 pixels/surface temperatures of substrate per image were acquired. The system was programmed to extract *SST* (300 pixels per image/seed tray) automatically from the original thermal image. All *SST* data were assigned with consecutive seed numbers in the seed tray (P_i (i = 1~300)) (Figure 2-2). Two kinds of experiments, either different 1) *SAT* or 2) *VPNS* during the germination stage for both U and C, were conducted. For the first experiment, different *SAT* every 4 °C from 12 to 40 °C with *VPNS* of 86% was identified; for the second experiment,

VPNS of 77%, 82%, and 86% with *SAT* of 20 °C was identified (Table 2-2).

Figure 2-5 shows the probability density function (PDF) of *GT* to 1) different *SAT* with *VPNS* of 86% (Figure 2-5a, b) and 2) different *VPNS* with *SAT* of 20 °C (Figure 2-5c, d), using 300 seeds of U and C, respectively. Variance of *GT* was found for both U and C in accordance with variable microenvironments, *SAT* and *VPNS*, and management factors (Figure 2-5). Earlier and uniform germination are beneficial for the consistent production. For this experiment, *SAT* of 24 °C with *VPNS* of 86% and management factor U showed the earliest and most uniform germination (Figure 2-5a).

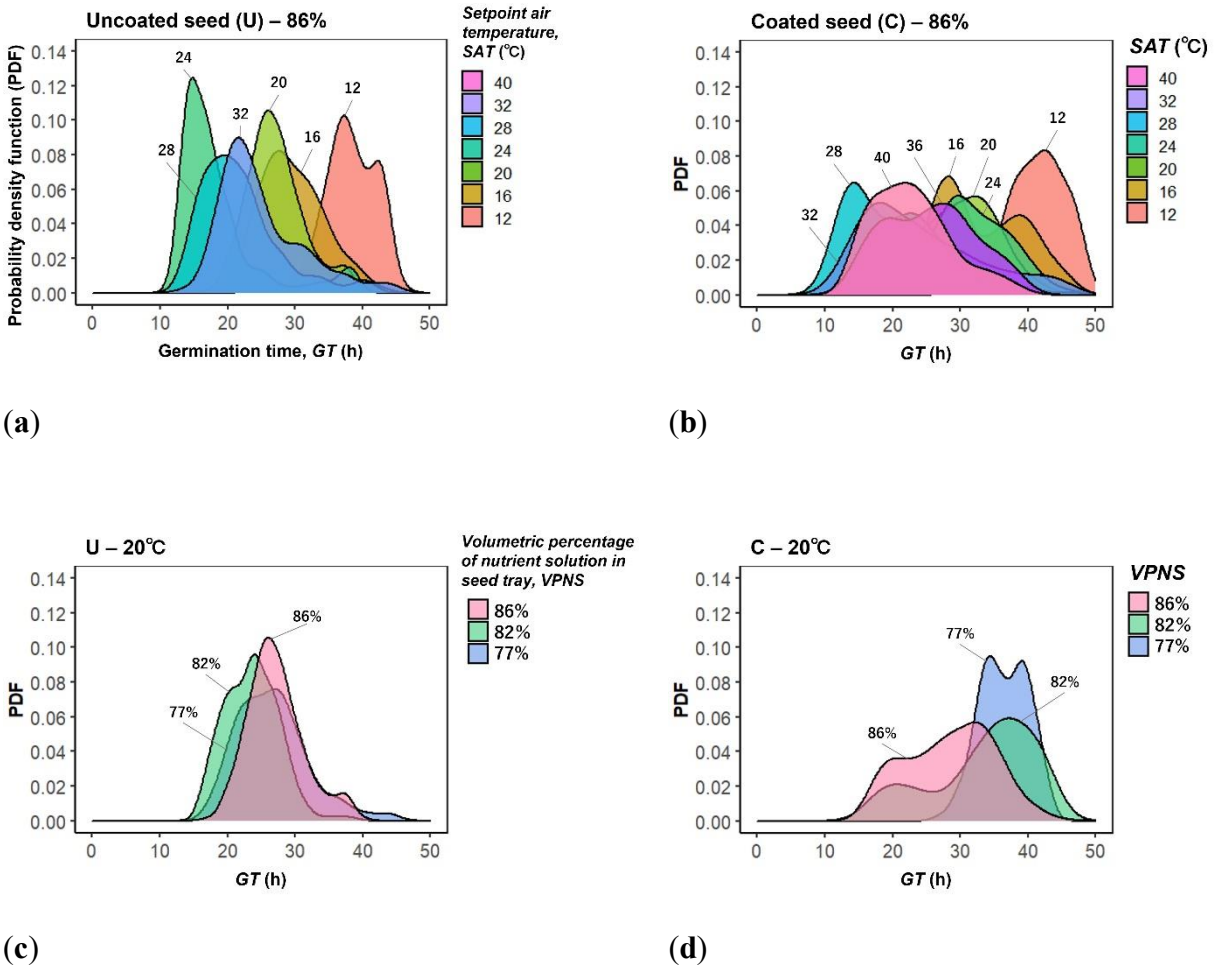

(**a**) (**b**)

(**c**) (**d**)

Figure 2-5. Probability density function (PDF) of germination time (*GT*) under 1) different setpoint air temperature (*SAT*) and volumetric percentage of nutrient solution in seed tray (*VPNS*) of 86% each with (a) uncoated seed—U and (b) coated seed—C, and 2) different *VPNS* and *SAT* of 20 °C with U (c) and C (d) (see Table 2-1 for abbreviations).

Figure 2-6 illustrates scatter diagrams of *GT* and *SST* under 1) different *SAT* with *VPNS* of 86% (Figure 2-6a, b) and 2) different *VPNS* with *SAT* of 20 °C (Figure 2-6c, d), each with both 300 of U and C. *GT* and *SST* of individual seeds were quantified in response to different *SAT*, *VPNS* and U/C (Figure 2-6). Variance of *GT* and *SST* differed depending on the microenvironment and management factor. In this experiment, for U with different *SAT* with fixed *VPNS*, overall germination was limited or not found with *SAT* of 36 °C and 40 °C (Figure 2-6a, Table 2-3).

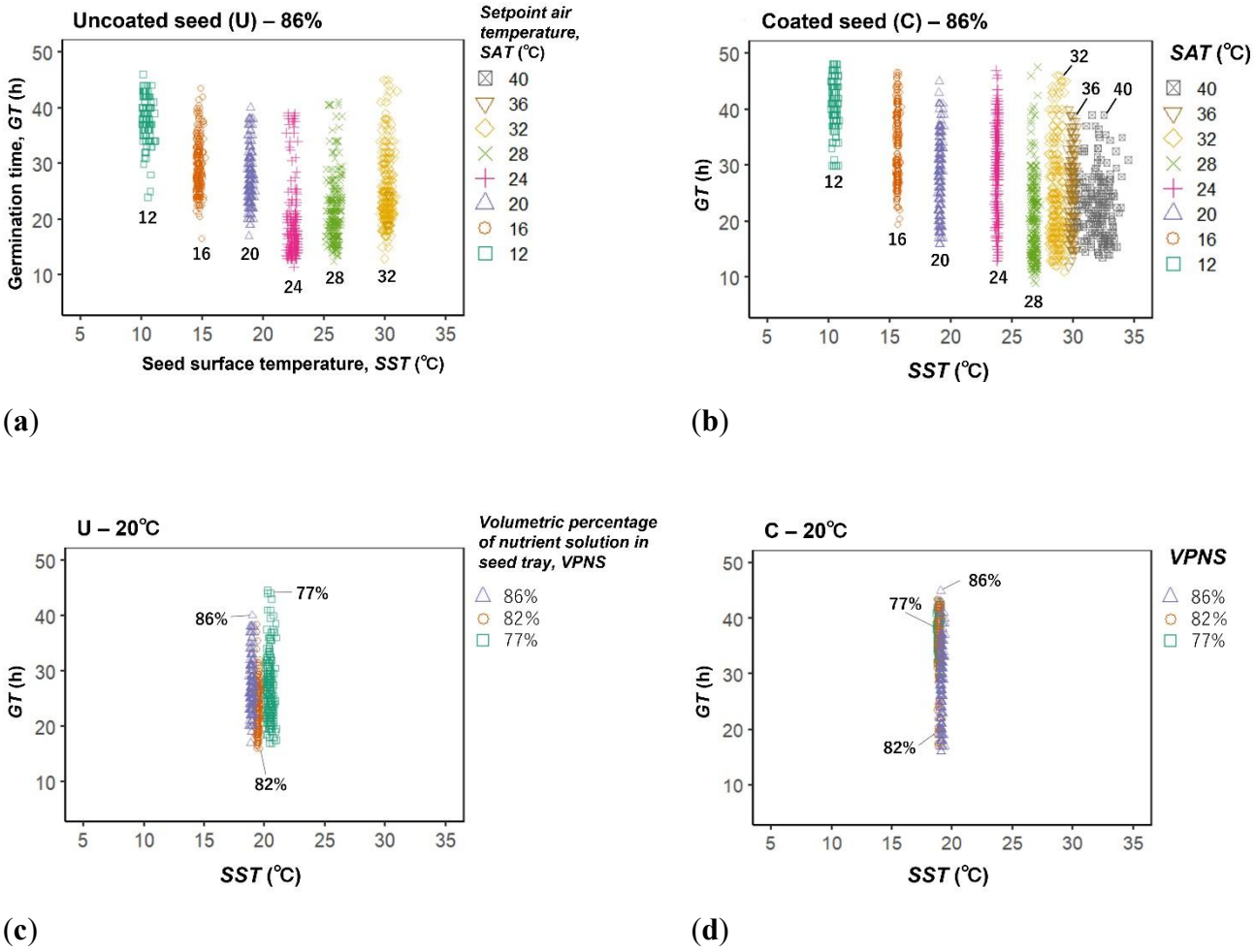

Figure 2-6. Scatter diagram of germination time (*GT*) and seed surface temperature (*SST*) under 1) different setpoint air temperature (*SAT*) and volumetric percentage of nutrient solution in seed tray (*VPNS*) of 86% each with 300 (a) uncoated seeds—U and (b) coated seeds—C, 2) different *VPNS* and *SAT* of 20 °C with U (c) and C (d). Each symbol

corresponds to one seed (see Table 2-1 for abbreviations).

Figure 2-7 describes $\overline{SST}$ and $\overline{AT}$ under different *SAT* (12, 16, 20, 24, 28, 32, 36, 40 °C) with *VPNS* of 86%, each with 300 of both U and C. For both U and C, $\overline{SST}$ was lower than *SAT* at higher *SAT*, especially of 36 °C and 40 °C, whereas $\overline{AT}$ remained closer to *SAT*.

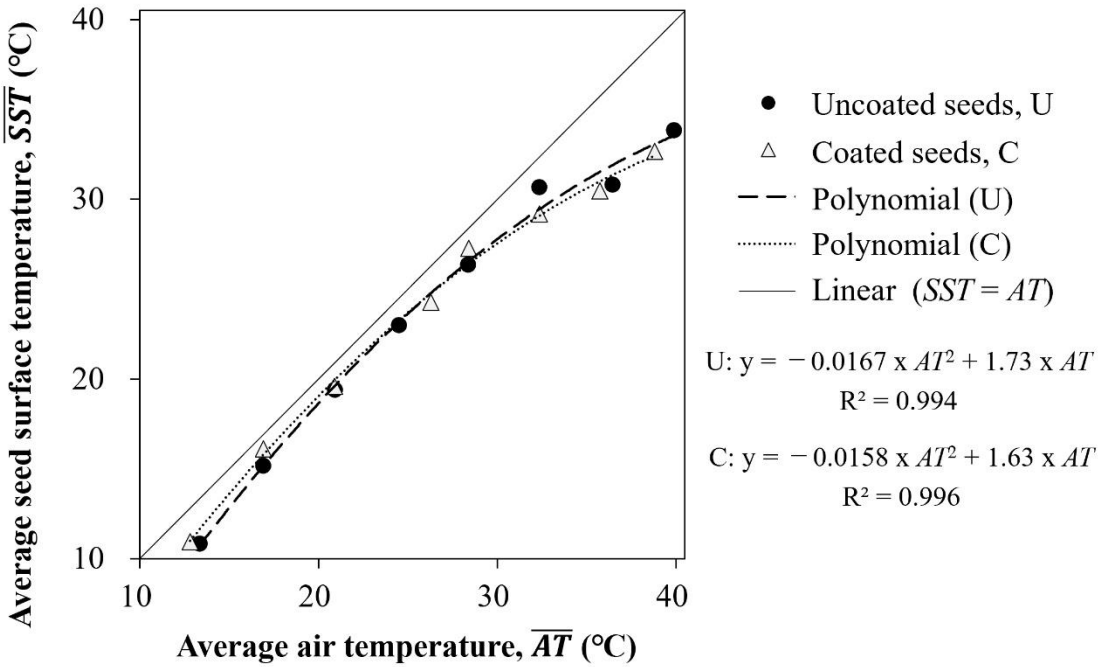

Figure 2-7. Average seed surface temperature ($\overline{SST}$) and average air temperature ($\overline{AT}$) under different setpoint air temperature (*SAT*) (12, 16, 20, 24, 28, 32, 36, 40 °C) and volumetric percentage of nutrient solution in seed tray (*VPNS*) of 86%, each with 300 uncoated seeds (U) and coated seeds (C). Some data of $\overline{AT}$ include the average temperature of a shorter time period than 48 h.

Table 2-3 shows $\overline{GT}$, $\overline{AT}$, $\overline{SST}$, *GP*, $\overline{GR}$, Identified percent, coefficient of variation of *GT* (*CVt*) and *SST* (*CVs*), each with different *VPNS*, *SAT*, and U/C. In addition to $\overline{GT}$, $\overline{SST}$ and $\overline{AT}$, *GP* was measured for each treatment. Identified percent is the percentage obtained by dividing the number of seeds of identified *GT* from RGB images by germinated seeds 48 HAS. The degree of uniformity of both *GT* and *SST* was

quantified with *CVt* and *CVs*, respectively. Furthermore, $\overline{GR}$ was calculated and indicated the difference in average germination rate for each condition.

Table 2-3. Average air temperature ($\overline{AT}$), average germination time ($\overline{GT}$), average seed surface temperature ($\overline{SST}$), germination percentage per 300 seeds 48 h after sowing (*GP*), Identified percent, and coefficient of variation of germination time (*CVt*) and seed surface temperature (*CVs*) together with average hourly germination rate per 300 seeds ($\overline{GR}$), each with different volumetric percentage of nutrient solution in seed tray (*VPNS*), setpoint air temperature (*SAT*), and uncoated seed (U)/coated seed (C). (See Table 1 for abbreviations).

Seed Type	*VPNS* (%)	*SAT* (°C)	Measured Value					Calculated Value		
			$\overline{AT}$ [1] (°C)	$\overline{GT}$ (h)	$\overline{SST}$ (°C)	*GP* (%)	Identified Percent [2] (%)	CVt $[St/\overline{GT}]$	CVs $[St/\overline{SST}]$	$\overline{GR}$ $[GP/\overline{GT}]$ (% h^{-1})
U	86	40	39.4	25.0	33.3	0	-	-	0.04	0.00
		36	35.9	21.8	30.3	1	67	0.2	0.02	0.05
		32	31.9	24.9	30.2	81	98	0.2	0.01	3.25
		28	27.9	21.7	25.9	100	83	0.3	0.01	4.60
		24	24.0	18.6	22.5	100	77	0.3	0.01	5.38
		20	20.4	27.2	18.9	100	90	0.2	0.01	3.68
		16	16.4	29.7	14.7	100	79	0.2	0.01	3.36
		12	12.9	38.2	10.4	100	46	0.1	0.02	2.62
	82	20	19.9	23.6	19.4	100	86	0.2	0.00	4.23
	77	20	20.0	26.7	20.4	100	89	0.2	0.01	3.74
C	86	40	38.3	22.8	32.2	91	62	0.3	0.03	3.98
		36	35.2	25.6	30.0	86	83	0.3	0.01	3.36
		32	31.9	24.3	28.7	79	97	0.4	0.01	3.24
		28	27.9	20.2	26.8	99	95	0.4	0.01	4.93
		24	25.8	29.2	23.8	100	99	0.2	0.00	3.42
		20	20.4	28.5	19.1	100	86	0.2	0.00	3.51
		16	16.4	33.0	15.6	100	81	0.2	0.01	3.02
		12	12.3	41.1	10.4	100	47	0.1	0.02	2.43
	82	20	19.9	33.4	18.9	100	42	0.2	0.01	3.00
	77	20	19.9	36.5	18.7	48	83	0.1	0.01	1.32

[1] Some data of $\overline{AT}$ include the average temperature of shorter time period than 48 h.

[2] *Identified percent*: percentage of identified *GT* from red-green-blue (RGB) images per germinated seeds 48 HAS.

$$St = \sqrt{\frac{1}{n}\sum_{i=1}^{n}(GT - \overline{GT})^2}. \quad (1)$$

2.4. Discussion

The objective of this study was to develop a plant phenotype measurement system to assess *GT* of individual seeds using time series data of 2D camera images and to analyze each *GT* as affected by its surrounding microenvironment and management factors of individual seeds for a wider plant cohort research project using the developed system. Experiments on germination were conducted to demonstrate the performance of the plant phenotype measurement system and its applicability for a whole plant growth process in a PFAL for large-scale commercial production and/or breeding.

Through the germination experiments of 1) different *SAT* with fixed *VPNS* and 2) different *VPNS* with fixed *SAT* each with U and C, *GT* of individual seeds were obtained from RGB images and were assessed for the effect of its surrounding microenvironment (*SST*, *VPNS*, and air temperature) and management factors (U and C) (Table 2-2). Our results together demonstrate the utility of the developed phenotyping unit for plant cohort research and future applications for further plant growth processes in PFAL for commercial production and/or breeding.

Traditional measurement of germination has been limited to the germination percentage of a seed population but not the germination time of individual seeds [49]. The result values of *GP* or $\overline{GT}$ shown in Table 2-3 represent an example of a previous germination measurement. Moreover, how microenvironment and management factors affect germination time of individual seeds and further plant growth had not been discussed in detail.

In this study, *GT* of individual seed could be obtained from time series data of 2D camera images, which were sent automatically and stored in the DWH together with other time course data captured from phenotyping and microenvironmental sensing units installed in GCB. Figure 6 illustrates *GT* of individual seeds sown in a seed tray each with 300 seeds under different treatments. Variance or uniformity of *GT* per 300 seeds was also demonstrated based on individual *GT* (Figure 2-5).

The results indicated that individual *GT* variations were affected by each microenvironment (*SST*, *VPNS*, and air temperature) and management factor such as seed type (U and C) (Figure 2-5, 2-6). Each treatment with different air temperature or

volumetric water/nutrient percent of the substrate, both with U and C, reflected the differing tendency of *GT* or variance of *GT*. In addition to microenvironmental factors, the results indicated that management factor (U and C) affected *GT*; *GT* itself and variance of *GT* varied in response to seed type (Figure 2-5, 2-6).

Furthermore, this experiment showed differing *GP*, particularly *SAT* of 36 °C and 40 °C, between U and C; little or no germination occurred with U, whereas *GP* with C and *SAT* of 36 °C and 40 °C were 86% and 91%, respectively (Table 2-3). This result indicates that C was less affected by microenvironment of higher air temperature. While on the other hand, with smaller volumetric percent in nutrient solution (*VPNS*), especially at 77% with *SAT* of 20 °C, values of $\overline{GT}$, *GP*, and $\overline{GR}$ were all smaller with C than U (Table 2-3). This implies that C was more affected by microenvironment of smaller volumetric water/nutrient percent of the substrate.

Figure 2-7 and Table 2-3 explained that under higher *SAT*, especially at 36 °C and 40 °C, $\overline{SST}$ was lower than the *SAT* by approximately 6 to 8 °C, whereas $\overline{AT}$ remained closer to *SAT* (even at higher *SAT*). This implies that it is critical to observe the microenvironment, and more attention should be paid to analyzing the relationship between various factors of microenvironment, management, and dynamic phenotypes.
As Figure 2-6 demonstrated individual *GT* under different microenvironments of *SST*, *VPNS* and air temperature together with management factors of U and C, it is presumed that some outliers of individual seeds can be found. Therefore, time series data of its surrounding microenvironment, management factors, and possibly genotype can be used to analyze what has generated the particular outliers [21]. Such analysis will also help to identify the causes of variation in seed germination time, which enables to remove the particular causes of variation [21].

We acknowledge that there are several limitations in this study. First, there were indeed limitations to determine *GT* from time series data of 2D camera images that were used for this study. By comparing with ground truth data on germination 48 HAS, *GT* of some germinated seeds were not obtained from the RGB images as shown with identified percent in Table 2-3. This challenge will be addressed in the future studies by improving the phenotyping unit and incorporating artificial intelligence (AI) in the system for

automated acquisition of *GT*.

Second, there is a possibility that the result was affected by additional microenvironment and management factors other than *SST*, *VPNS*, air temperature, and seed type. In particular, inclination of water surface, which was possibly caused by procedures for manually carrying the seed tray or soaking substrate in the water/nutrient solution, may have caused variation or 2D horizontal distribution of *SST*. For the future study, 2D horizontal distribution should be taken into account to analyze the effect of microenvironment and management factors. The 2D horizontal distribution of individual phenotype, microenvironment and management, such as water/nutrient solution, light, substrate, and other factors, may occur particularly with further plant growth [21].

Third, seed lots used for this study were different for each seed type of U and C. Ideally, the same seed population/lot should be used to compare the effect of management factor. In the future study, with the breeding and seed production in PFAL, this issue should be overcome by also tracing the seed production process and treatments.

In this study, the developed plant phenotype measurement platform revealed the effects of microenvironment and management factors on *GT* of individual seeds for plant cohort research. This indicates possibility of contributing to increasing in growth rate, plant quality and uniformity in plant production. In the future studies, additional conditions with multiple varieties/genotypes will be tested with this system. For the plant cohort research in PFALs, further study on plant growth stage is expected to continuously analyze individual phenotypes together with plant communities to assess interactions of plant phenotype dynamics with microenvironment, management, and genotype for life cycle history of individual plants to improve productivity of plant production and breeding in PFALs.

2.5. Conclusions

In this study, plant phenotype measurement system was developed to assess *GT* of individual seeds, using time-series 2D camera images, and to analyze how microenvironment and management factors affect the *GT* for plant cohort research. In particular, the low cost and compact modular system designed in this study emphasizes

the practicality and scalability in commercial plant production in PFALs. Using this system, germination experiments were conducted to demonstrate the performance of the system and its applicability for a whole plant growth process in a PFAL for commercial production and/or breeding.

Through this study, *GT* of individual seeds were obtained from time series 2D camera images by using the developed modular plant phenotype measurement system as an initial stage of the plant cohort research in PFALs. Furthermore, the phenotyping platform revealed the effects of microenvironment and management factors on *GT* of individual seeds. Our modular plant phenotype measurement system should advance the commercial plant production in PFALs.

Chapter 3. Variations in the growth of cotyledons and initial true leaves as affected by photosynthetic photon flux density at individual seedlings and nutrients

3.1. Introduction

Plant factories with artificial lighting (PFALs), with an almost airtight and well-insulated structure, have the potential to enable the production of large quantities of high-quality plants year-round while achieving high efficiency of resource utilization [1–11]. The theoretical benefits of PFAL can be achieved only when the system is properly engineered, constructed, and operated [18–20]. In actuality, a variety of PFAL challenges remain, including high initial investment, optimal cultivation system, and environmental controls, which can be solved by improving productivity in PFALs [20].

Despite the controlled environment in PFALs, variations in plant individuals have been found, particularly around harvesting, which results in a negative effect on plant productivity in PFAL operations [6,11,21,22]. The uniformity of plant growth by reducing two-dimensional (2D) variations in plant traits (i.e., phenotype), such as fresh weight, plant height, morphology, and concentrations of secondary metabolites per plant, can contribute to productivity improvement in PFALs [21]. Variations in the plant traits of individual plants are mainly ascribed to three factors: environment, genotype (species and cultivar), and management (human and machine intervention) [6,11,21]. Indeed, 2D variations in plant traits over a cultivation tray are partly attributed to 2D variations in the surrounding microenvironment of individual plants, including photosynthetic photon flux density (PPFD) and air current speed over and within the plant canopy or individuals in the tray [21]. Past studies have shed light on the PPFD distribution in the cultivation tray, and even the difference in the PPFD distribution between a plant canopy and the cultivation tray without plants [24–26].

Plant phenotyping plays an integral role in understanding how the microenvironment surrounding individual plants affects variations in the phenotype of individual plants [6,11,21,32]. Plant phenotyping is a set of methodologies and protocols used to study plant performance, growth, architecture, and composition at different scales

of organization, from organs to canopies, and it elucidates the plant trait dynamics in a non-destructive and non-invasive manner [6,11,21,32–34]. Having great potential for application to commercial PFALs [38], image-based studies in PFALs have been conducted, including quantifying the projected leaf area (value measured by 2D camera images captured from above the plant canopy or seedling trays) of the plant canopy [22,39–44].

Cotyledons are the first leaves that appear on a plant and play a crucial role in the development of seedlings, particularly in the early stages, which affects the subsequent plant growth process [28–31]. During the initial growth stage of leaf development, leaf tissues are built and require carbon and energy from other parts of the plant [60,61]. At the seedling stage, plants are dependent on the immediate establishment of photosynthesis, leading to shoot development, which mainly depends on the photosynthetic capacity of the cotyledon and stored nitrogen [61]. Early photosynthesis by the cotyledon is essential for seedling growth [31]. Therefore, to achieve maximal plant growth, PPFD and nutrient availability are environmental factors that strongly affect plant growth from the early developmental stages of seedlings onwards [61,62].

However, most previous studies on the cotyledon and initial stage of seedlings have been limited to the mean values of plant population, not the individual plants, alongside average PPFD, not the PPFD at individual plants. Furthermore, most image-based analyses or quantification of the projected leaf area of seedlings in PFALs have been conducted only after the emergence of true leaves. The frequency of image capture has been confined to a few times per day or even per week. Therefore, to elucidate the variations in the growth of cotyledons and initial true leaves, and how this is affected by the PPFD and nutrients, which are the essential factors for the initial development of plants, it is crucial to measure cotyledon unfolding time and the time series projected leaf area together with ground truth measurements, and analyze how the microenvironment of PPFD at individual seedlings and nutrients affects individual growth.

A modular plant phenotype measurement system for seedling production was developed, focusing on practicality and scalability in commercial PFALs, and achieved low cost using small cameras and sensors, and a cultivation method similar to that of

commercial PFALs. In this study, the initial stage of seedlings, one of the critical early stages of plant growth, was used as part of research that examined the entire plant life cycle. Experiments were conducted to obtain cotyledon unfolding time and the time series projected leaf area of cotyledons and true leaves of individual seedlings of romaine lettuce (*Lactuca sativa* L. var. longifolia), using 2D camera images. This was also undertaken to analyze how the surrounding microenvironment of PPFD and nutrients affects the variations in the growth of individual seedlings for plant cohort research. Considering leaf movement [22,63,64], red-green-blue (RGB) images were acquired and processed every 0.5 h.

In plant cohort research, the life cycle phenome history of individual plants can be captured continuously and noninvasively, and analyzed from seed sowing to harvesting using phenotyping units, together with the time series data on environment, managemental, and resource inputs and outputs in PFALs [4–6,11,21,47]. Using the time series datasets in the data warehouse, plant cohort research makes it possible to identify optimal set points of environmental factors for maximizing multi-objective functions and concurrently improving plant productivity, selection of seedlings for grading, and breeding new cultivars in PFALs [4–6,11,21,47].

Through this study, cotyledon unfolding time and the time series projected area of cotyledons and true leaves of individual seedlings were obtained, using time series RGB images. In agreement with the actual individual measurements, variations in seedling growth were identified, even under similar microenvironments. Furthermore, the results demonstrated larger variations in seedlings with higher relative growth.

3.2. Materials and Methods

3.2.1. Description of the System

A modular seedling production system (MSPS) was developed by improving the germination container box (GCB) equipped with a phenotyping unit and air temperature and relative humidity sensors [6] as a serial study for plant cohort research in PFALs. Figure 3-1 shows a configuration diagram of the MSPS composed of eight units and parts. The additionally installed items in the GCB included LEDs, an air circulator, and a digital

weight scale with data loggers (L, M, and N, respectively; Figure 3-1).

The phenotyping units, sets of RGB cameras (Raspberry Pi Pi NoIR Camera Module V2; Raspberry Pi Foundation, Cambridge, UK) (×4), and white LEDs for the flash of the RGB cameras (15 white LED tape, length 300 mm; SOF-15W-30-3SMD; Tokulumi Co., Ltd., Kwai Chung, Hong Kong) (×4) [6] were set 485 mm above the surface of each seedling tray (E and F, respectively; Figure 3-1). Additionally, four air temperature and relative humidity (*Tin* and *RH* respectively) sensors were placed 50 mm above the right or left of the surface of the seedling trays. The phenotyping unit, consisting of RGB cameras and white LEDs for the flash, and *Tin* and *RH* sensors were connected to each control board (Raspberry Pi 3 Model B; Raspberry Pi Foundation, Cambridge, UK) (×4), and activated every ten minutes [6]. These data were automatically sent to a data warehouse (DWH) through control boards [6,56].

Seedling trays were placed consistently at each designated location. For this study, two trays on the right side (Trays 1 and 2) of four in the MSPS were used, and the remaining two trays on the left (Trays 3 and 4) were also filled with the same plants simultaneously for another analysis (Figure 3-1).

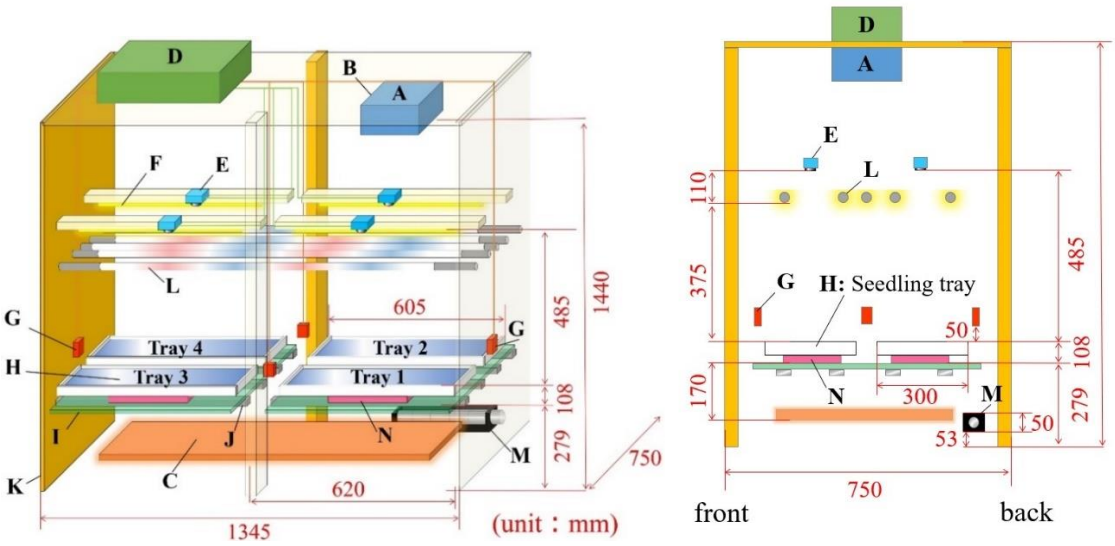

(a) **(b)**

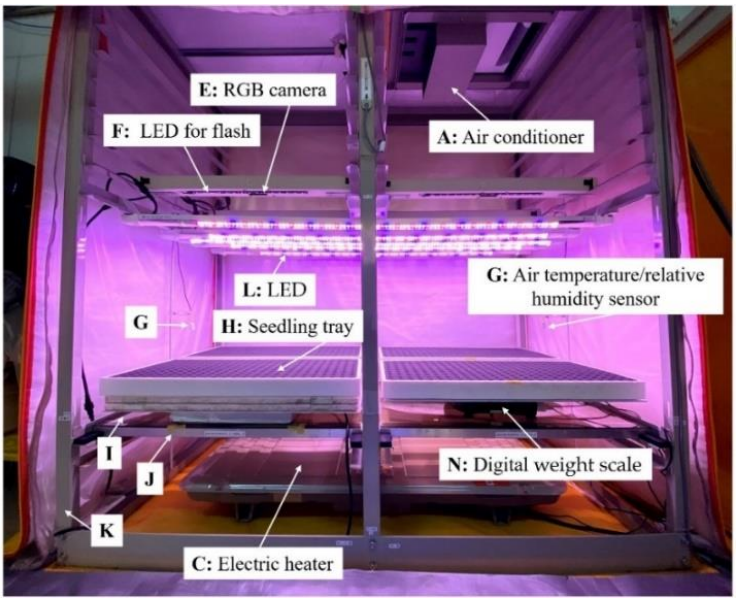

(c)

Figure 3-1. Modular seedling production system (MSPS) equipped with phenotyping unit and air temperature and relative humidity sensors. (a) Schematic diagram. (1) Temperature control unit: air conditioner (A), air outlet of the air conditioner (B), electric heater (C). (2) Phenotyping unit: control board (×4) (D), red-green-blue (RGB) camera (×4) (E), white light-emitting diode (LED) for flash (×4) (F). (3) Air temperature and relative humidity sensor (×4) (G). (4) Cultivation unit: seedling tray with the substrate (seedling tray) (×4) (H), acrylic plate (I), reinforcement bar (J). (5) Exterior box with frame (K). [6] (6) LED (18 W each, length 1170 × width 30 × height 25 mm) (ZK-TB18-VE02/A; Fujian Sanan Sino-Science Photobiotech Co., Ltd., Fujian, China) (×5) (L). (7) Air circulator (DC12V 0.2A, blade size: 30 × 190 mm, length 240 × width 48 × height 50 mm) (a15110600ux0249jp; Uxcell, Hong Kong, China) (M), and (8) digital weight scale (linearity error ± 300 mg, precision 100 mg) (×3) with data loggers (×2) (N). (b) Schematic diagram from the side. (c) Inside view of MSPS.

3.2.2. Light Environment for Individual Seedlings

To study the growth variations in the seedlings as affected by the PPFD, a light environment was designed to maximize the distribution of horizontal PPFD over the seedling tray in conjunction with minimizing the PPFD variations between the two seedling trays (Tray 1 with the water and Tray 2 with the nutrient solution (nutrients)) (Figure 1a, Table 1). Therefore, to set the desired PPFD distribution over the tray, both side edges of five LEDs, except the one in the middle, were covered with aluminum tape.

First, each seedling tray (605 × 300 × 42 mm), having a black substrate inside 300 plants (tray), was divided into 18 sections. Then, horizontal PPFD 0.04 m above the surface of the tray was measured at each section using PPFD sensors (accuracy ± 5 %) (LI-190R; LI-COR, Inc., Lincoln, NE, USA) with a data logger. The distributions of horizontal PPFD within the trays are shown in Table 3-1: from the minimum 84 to the maximum 205 (Tray 1) or 208 (Tray 2) μmol m^{-2} s^{-1}. The 18 different PPFDs in each tray were categorized into three classifications (6 PPFDs/classification) based on the level of PPFD: low (L), medium (M), and high (H), as 84 ≤ 126, 126 < 166, and 166 ≤ 208 μmol m^{-2} s^{-1}, respectively (Table 3-1).

For the experiments, two representative plants from 16 or 20 plants in each section closest to the PPFD sensor were chosen (2 × 18 PPFDs/tray × 2 = 72 representative plants). Therefore, there were 12 representative plants for each treatment (2 × 6 PPFDs/treatment × 3 PPFD classifications × 2 (nutrients/water) = 72 representative plants) (Table 3-1). If the representative plants did not germinate, the plants next to the original representative plants were selected. The remaining seedlings, other than 72 representative plants, were also cultivated together, as there were 300 plants in each tray, following a cultivation method similar to that used for commercial PFALs. The average ratio of the LED spectrum, blue: green: red: far-red, at the trays, was 13:16:60:11.

Table 3-1. Treatments and codes of the experiment. The distributions of horizontal PPFD within the trays (width 605 × length 300 mm) were set for this study. Here, 18 different PPFDs in each tray (Tray 1 with the water and Tray 2 with the nutrients) were categorized into three classifications (6 PPFDs/classification) based on the level of PPFD: low (L), medium (M), and high (H), 84 ≤ 126, 126 < 166, 166 ≤ 208 μmol m^{-2} s^{-1}, respectively.

Code	Nutrients/Water	PPFD classifications	Distribution of horizontal PPFD (μmol m^{-2} s^{-1})
Nutrients-H	Nutrients (Tray 2)	High	175, 181, 187, 195, 202, 208
Nutrients-M		Medium	140, 145, 147, 148, 151, 165
Nutrients-L		Low	84, 102, 102, 104, 118, 126
Water-H	Water (Tray 1)	High	168, 175, 181, 190, 197, 205
Water-M		Medium	136, 142, 144, 148, 153, 161
Water-L		Low	84, 100, 104, 112, 121, 123

3.2.3. Hours to Cotyledon Unfolding and Projected Area of Cotyledon and True Leaves of Individual Plants Estimated with Time Series RGB Images

In this study, an RGB camera was used to obtain 2D image data every 0.5 h to estimate the hours required for cotyledon unfolding (*Hc*: the time from sowing to the unfolding of the cotyledon of individual plants) and the time course of the projected area of the cotyledon (*Ap-c*), true leaf (*Ap-t*), and cotyledon and true leaf (*Ap-ct*) of individual seedlings at intervals of 0.5 h (See Table 3-2 for abbreviations). In the case of a failure of image capturing, the RGB image acquired ten minutes before the scheduled timing was used because the raw image data were automatically captured every ten minutes.

Each RGB image, which covered one tray with 300 seedlings, was first divided into 18–300 images depending on the size of the seedlings for ease of image processing. Then, the time series RGB images of each seedling were re-sequenced in chronological order with 0.5 h intervals [6] (Figure 3-2a).

To estimate *Hc*, the first RGB image with a clearly visible unfolded cotyledon, which achieved the most horizontal position, was selected among the time-course images of individual seedlings in chronological order [6]. Then, to estimate the projected areas of cotyledons and true leaves, each RGB image of individual seedlings, in chronological order, was imported into graphic editor software (Photoshop, Adobe Inc., San Jose, CA, USA) to carefully eliminate the background from the image so that only time series

images of cotyledons and true leaves remained (Figure 3-2b). The backgrounds of individual cotyledons and true leaves were carefully eliminated with zoomed images, particularly in the case of overlapping leaves and the attached seed coats, as coated seeds were used in this study (Figure 3-2a, b). Furthermore, time series images of cotyledons and true leaves were divided into different images so that *Ap-c* and *Ap-t* could be estimated separately (Figure 3-2a, b).

To estimate *Ap-c* and *Ap-t*, ImageJ, a Java-based open software package for image processing, was used [65]. Before importing the edited images, the scale was set by associating the distance in pixels with the actual distance between each substrate hole in the raw images. The scale was selected based on the number of pixels per millimeter. The edited time series images were processed into binary images, and the threshold was set to acquire the projected areas. Separated time series *Ap-c* and *Ap-t* of the individual seedlings were estimated, along with *Ap-ct*, the sum of individual *Ap-c* and *Ap-t*. To identify the accuracy of horizontal projected leaf areas that were possibly affected by the camera angle of view, 52 same-sized square pieces of paper, as a substitute for the plants, were placed horizontally in the tray in an equidistant manner, and the RGB images were captured. The accuracy of the 52 area values using ImageJ among the tray was ± 5%. In this study, the projected images obtained from a single RBG camera covering one tray were used without adjusting the viewing angle or distortion correction, which possibly affected the estimation of some projected areas of the inclined leaves.

For the ground truth measurement, ImageJ was used to estimate areas of the cotyledons (*Ac*), true leaves (*At*), and cotyledons and true leaves (*Act*) of the individual seedlings 216 h after sowing (HAS) (See Table 3-2 for abbreviations). Separated cotyledons and true leaves of individual plants 216 HAS laid on the whiteboard together with a ruler were photographed manually with a camera (α 6000; SONY Corp., Tokyo, Japan) set at 0.675 m above the board, while maximizing the magnification of the lens.

The exact process for the projected areas was also carried out to estimate *Ac*, *At*, and *Act*, except for the scale setting process, in which the scale of a ruler was associated with the number of pixels per mm. Note that petioles of both cotyledons and true leaves of individual plants were not included in *Ap-c, Ap-t*, *Ap-ct*, *Ac*, *At*, and *Act*.

3.2.4. Experimental Design

3.2.4.1. Plant Material and Culture Conditions

To analyze the variations in the growth of cotyledons and initial true leaves as affected by PPFD at individual plants and the nutrients, experiments on seedlings were conducted from cotyledon unfolding to 216 HAS. Coated seeds of romaine lettuce (*Lactuca sativa* L. var. longifolia, Lomaria, TLE487, Takii & Co., Kyoto, Japan) were used. The average weight and percentage of dry matter of 100 uncoated seeds of the same variety were 1.4 mg and 92%, respectively. Black substrates made of flexible polyurethane foam (MIRAI Co., Ltd., Kashiwa, Japan, 584 × 280 × 28 mm, 300 wells, 12 mm in diameter × 6 mm deep) were used in the cultivation trays. Instead of the white substrate, a black substrate was chosen for this study to prevent light reflection from the surface of the substrate to the backside of the leaf surface.

The photoperiod was set to an average of 16 h per day. In addition to the light for cultivation, flashes for the RGB camera were set to 10 s/time for photographing every 10 min. Regarding the nutrient solution, Chiba University's lettuce formula [59] was used, with pH and electrical conductivity of 6.5 and 0.19 S m^{-1}, respectively. The volumetric percentage of the nutrient solution or water in the tray was 86% [6].

The air temperature inside the MSPS was set to 20 °C during the experimental period. Average *Tin* and *RH* ($\overline{Tin}$, $\overline{RH}$) during the photoperiod and dark period over 9 days were 21 ± 0.2 °C and 85 ± 2%, and 21 ± 0.6 °C, and 92 ± 2%, respectively. CO_2 concentrations during the photoperiod inside the MSPS were maintained at 1500 ± 50 μmol mol^{-1}. Air current speed 0.05 m above the surface of the trays was 0.16 ± 0.11 m s^{-1}, measured with a hot-wire anemometer (accuracy ± 2% or 0.02 m s^{-1}) (6531-21; KANOMAX JAPAN Inc., Suita, Osaka, Japan).

The MSPS was placed inside an environmentally controlled cultivation room under the hygienic conditions of PFAL at the Kashiwanoha Campus of Chiba University. The air temperature, relative humidity, and CO_2 concentrations inside the cultivation room were 20 °C, 80–100%, and 1470 ± 20 μmol mol^{-1}, respectively.

3.2.4.2. Data Acquisition, variables and symbols

During the 9 days of cultivation, each RGB camera obtained 432 images (216 h × 0.5 h) per tray to estimate *Hc* and the time course of *Ap-c*, *Ap-t*, and *Ap-ct*. The time series projected areas of cotyledons and true leaves every 0.5 h of 72 seedlings (2 representative plants/the same PPFD × 18 different PPFDs × 2 trays either with the nutrients or the water) were estimated from cotyledon unfolding to 216 HAS. In total, approximately 300 (150 h × 0.5 h) time series projected areas per seedling were estimated, about 600 for both cotyledons and true leaves per seedling; thus, 43,200 projected areas for 72 seedlings.

In addition to the time course of the projected areas, actual manual measurements of 72 seedlings were individually conducted 216 HAS. As described in Table 3-2, in addition to *Ac*, *At*, and *Act*, shoot (cotyledon, true leaves, hypocotyl, and petiole) fresh weight, shoot dry weight (*Wf* and *Wd*, respectively), and hypocotyl length (*Lh*) were measured for each seedling 216 HAS. *Wd* was quantified after drying for two days at 80 °C in a thermostatic oven (accuracy ± 1 °C) (WFO-520W; TOKYO RIKAKIKAI Co., Ltd., Bunkyo-Ku, Tokyo, Japan). For weight measurement, a digital scale was used after calibration (linearity error ± 0.2 mg, precision 0.1 mg). A vernier caliper (instrumental error ± 0.03 mm) was used to measure *Lh*.

Additionally, the ratio of *Act* to *Wd* (*Act* divided by *Wd*) was calculated. To assess growth variations, the growth of each seedling was quantified and analyzed to determine how it was affected by the microenvironment of 18 different PPFDs, during both the photoperiod and dark period, and the nutrients or water. Horizontal integrated PPFD during hours from cotyledon unfolding (*Hc*) to 216 HAS of the individual plants (integrated PPFD) was also calculated for the analysis.

Table 3-2. List of symbols, variable names with descriptions and units.

Symbol	Variable name/Description	Unit
Ac, $\overline{Ac}$	Cotyledon area of individual plant 216 h after sowing (HAS), and their average	mm^2
Act, $\overline{Act}$	Area of cotyledon and true leaves of individual plant 216 HAS, and their average	mm^2
At, $\overline{At}$	True leaf area of individual plant 216 HAS, and their average	mm^2
Ap-c, $\overline{Ap-c}$	Projected cotyledon area of individual plant, and their average	mm^2
Ap-ct, $\overline{Ap-ct}$	Projected area of cotyledon and true leaves of individual plant, and their average	mm^2
Ap-t, $\overline{Ap-t}$	Projected true leaf area of individual plant, and their average	mm^2
Hc, $\overline{Hc}$	Hours to cotyledon unfolding (from sowing to the unfolding of the cotyledon) of individual plant, and their average	h
LAR	The ratio of leaf area (*Act*) to shoot dry weight (*Wd*) (*Act* divided by *Wd*)	$m^2\ g^{-1}$
Lh, $\overline{Lh}$	Hypocotyl length of individual plant 216 HAS, and their average	mm
Integrated PPFD	Integrated PPFD during hours from cotyledon unfolding (*Hc*) to 216 HAS of individual plant	$mol\ m^{-2}$
PPFD	Horizontal photosynthetic photon flux density at individual plant 0.04 m above the surface of the tray	$\mu mol\ m^{-2}\ s^{-1}$
VPNS	Volumetric percentage of nutrient solution in the tray [6]	%
Wd, $\overline{Wd}$	Shoot (*ct, h,* and petiole) dry weight of individual plant 216 HAS, and their average	mg/plant
Wf, $\overline{Wf}$	Shoot fresh weight of individual plant 216 HAS, and their average	mg/plant

3.3. Results

In this study, image data having an interval of 0.5 h were used to estimate *Hc* and projected areas of *Ap-c*, *Ap-t*, and *Ap-ct*. Figure 3-2 shows time series images of the same seedling in chronological order from 125 to 216 HAS as a case example among 72 seedlings. The seedling in Figure 3-2, with Nutrients-H (202 $\mu mol\ m^{-2}\ s^{-1}$), achieved the largest *Ap-ct* among 72 seedlings 216 HAS. Figure 3-2 shows time series RGB images in chronological order, time series images of cotyledon, and time series images of true leaf after its emergence. Additionally, magnified images of the same seedling 216 HAS: RGB image, cotyledon, and true leaf after removing background, and separated images of cotyledon and true leaf are shown in Figure 3-2b.

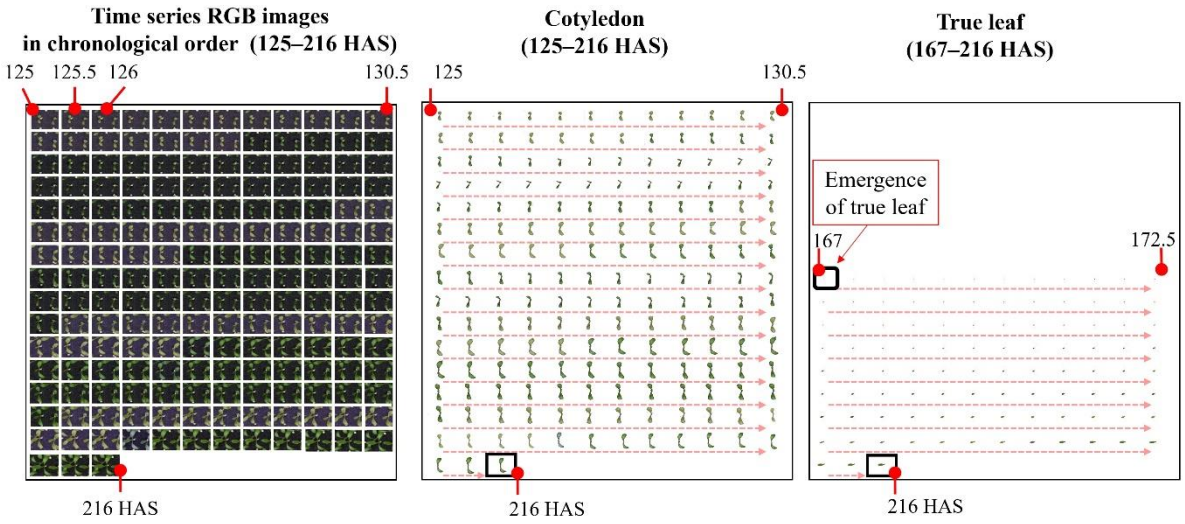

(**a**)

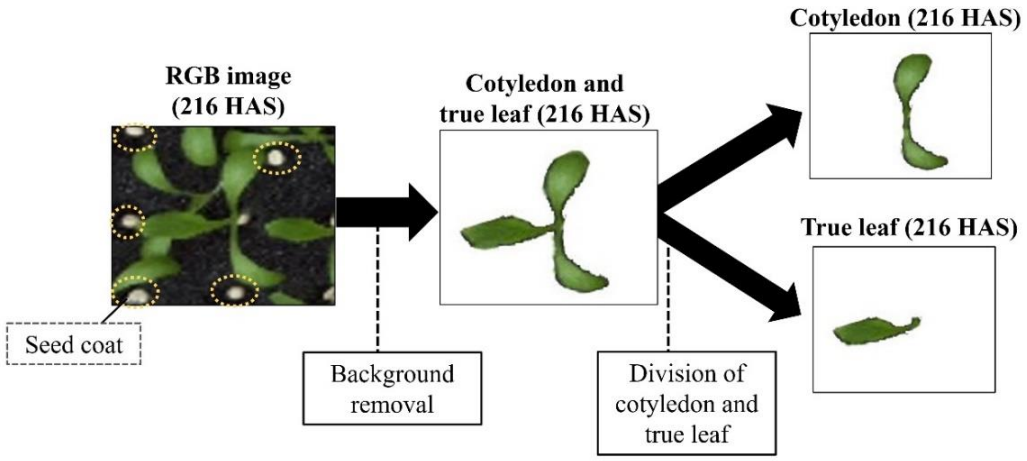

(**b**)

Figure 3-2. The time series RGB images of the same seedling, in chronological order, at 0.5 h intervals from 125 to 216 hours after sowing (HAS). This seedling, with nutrients and at high PPFD levels (Nutrients-H) (202 μmol m^{-2} s^{-1}), reached the largest projected area of cotyledon and true leaves among others 216 HAS. (a) Time series RGB images, time series images of cotyledon, and time series images of true leaf after its emergence. The cotyledon unfolding time was 66.5 h. (b) Magnified images of the same seedling at (a) 216 HAS: RGB image, cotyledon, and true leaf after background removal, and separated images of cotyledon and true leaf.

To analyze the variations in the growth of cotyledons and initial true leaves as affected by horizontal PPFD at individual seedlings and nutrients and water, experiments

on the initial stage of seedlings were conducted from cotyledon unfolding to 216 HAS. For the microenvironmental data, horizontal PPFD 0.04 m above the surface of the tray at individual seedlings was measured (Table 3-1). Two seedling trays, together with either nutrients or water, were used, each with 18 different PPFDs ranging from 84 to 205 or 208 μmol m^{-2} s^{-1} (Table 3-1). In addition to the time course of the projected areas, actual manual measurements of 72 seedlings were individually conducted 216 HAS.

Figure 3-3 shows *Hc* and *Wd* of individual seedlings with nutrients and water. In this study, no specific effect of *Hc* on *Wd* was found, as illustrated in Figure 3-3. Most of the individuals resulted in an *Hc* of 63–70 h, except three seedlings with water that had *Hc* values of 77.5, 78.5, and 79 h, which led to the maximum 16 h difference between the largest and the smallest *Hc* (Figure 3-3). It appeared that even the majority of *Hc* (63–70 h) varied by a maximum of 7 h, although this occurred during the dark period in this study. The average *Hc* ($\overline{Hc}$) was 66.2 h with nutrients and 68 h with water; $\overline{Hc}$ with nutrients was 1.8 h shorter than that with water.

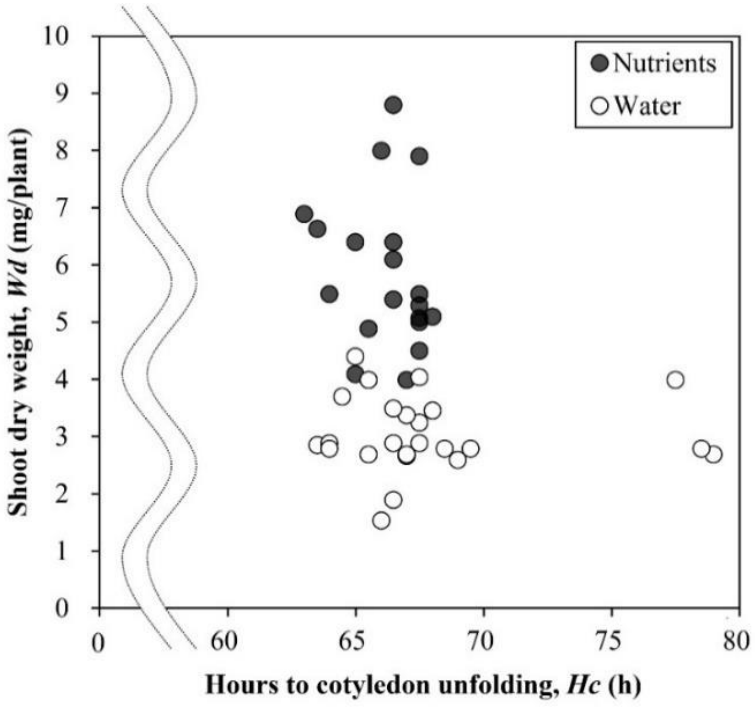

Figure 3-3. Hours to cotyledon unfolding (from sowing to the unfolding of the cotyledon) of individual plants (*Hc*) and shoot (cotyledon, true leaves, hypocotyl, and petiole) dry weight of individual plants 216 h after sowing (HAS) (*Wd*) with nutrients and water.

Figure 3-4 illustrates the time course of the *Ap-c* and *Ap-t* of individual seedlings, both with nutrients and water from *Hc* to 216 HAS, each with distributions of horizontal PPFDs (see Table 3-1 for treatments and codes). Note that some of the *Ap-c* or *Ap-t* at specific periods were not estimated because of the overlapping of the leaves. For some seedlings *Hc* could not be calculated, and the polygonal lines started 66.5 or 68 HAS with nutrients and water, respectively, in response to each $\overline{Hc}$.

By estimating the projected areas of cotyledons and true leaves of individual seedlings separately, we demonstrated time-course changes of *Ap-c* and *Ap-t*, respectively (Figure 3-4). The relative changes over time in projected areas within the single seedlings suggested the time series movement of cotyledons and true leaves, including changes in leaning or direction, in addition to the relative growth, depending on the viewing angle of the camera.

Figure 3-5 shows the time-course increase in the *Ap-c* and *Ap-t* of individual seedlings, both with nutrients and water from *Hc* to 216 HAS, each with distributions of horizontal PPFDs (see Table 3-1 for treatments and codes). Although *Ap-c* and *Ap-t* with water remained reasonably constant over time, it caused a significant and continued increase in *Ap-c* and *Ap-t* with nutrients with more fluctuation over time. Indeed, a significant increase was found, especially in *Ap-t* with nutrients. Furthermore, *Ap-c* with nutrients continued to increase even after the initial development of *Ap-t* (Figures 3-4, 3-5). It appeared that, particularly for *Ap-c*, a relative increase was caused mainly in the dark period, not the photoperiod (Figures 3-4, 3-5). As clearly shown in Figures 3-4 and 3-5, this indicated a condition in which the relative growth in *Ap-c* and *Ap-t* was more extensive with a higher PPFD with nutrients. However, it was found that the time-course changes of individual seedlings with nutrients showed more considerable variations, compared to water (Figures 3-4, 3-5).

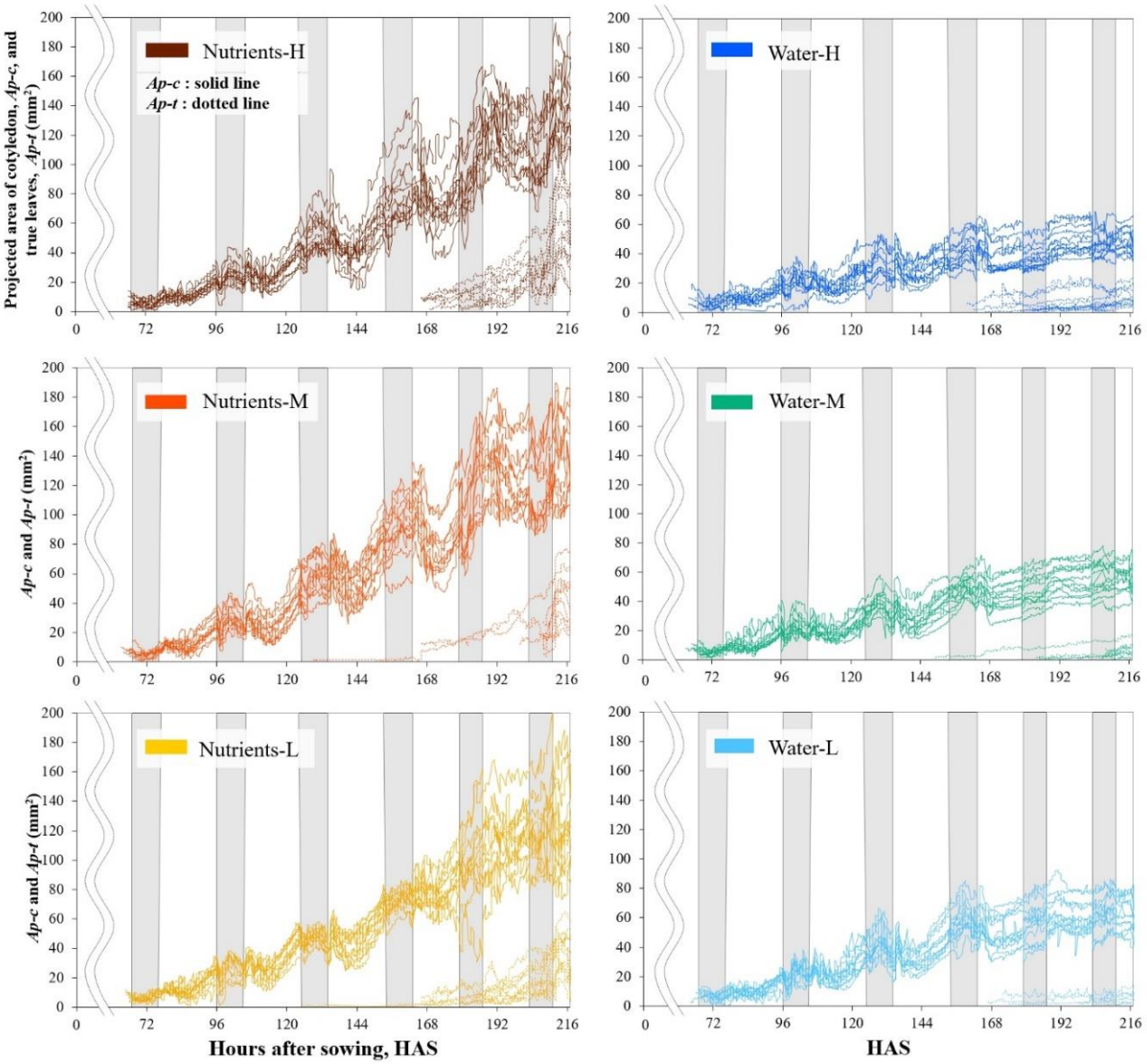

Figure 3-4. Time-course projected areas of the cotyledon (*Ap-c*) and true leaves (*Ap-t*) of individual seedlings with nutrients and water from hours to cotyledon unfolding from sowing (*Hc*) to 216 h after sowing (HAS), each with distributions of horizontal PPFDs (see Table 3-1 for treatments and codes).

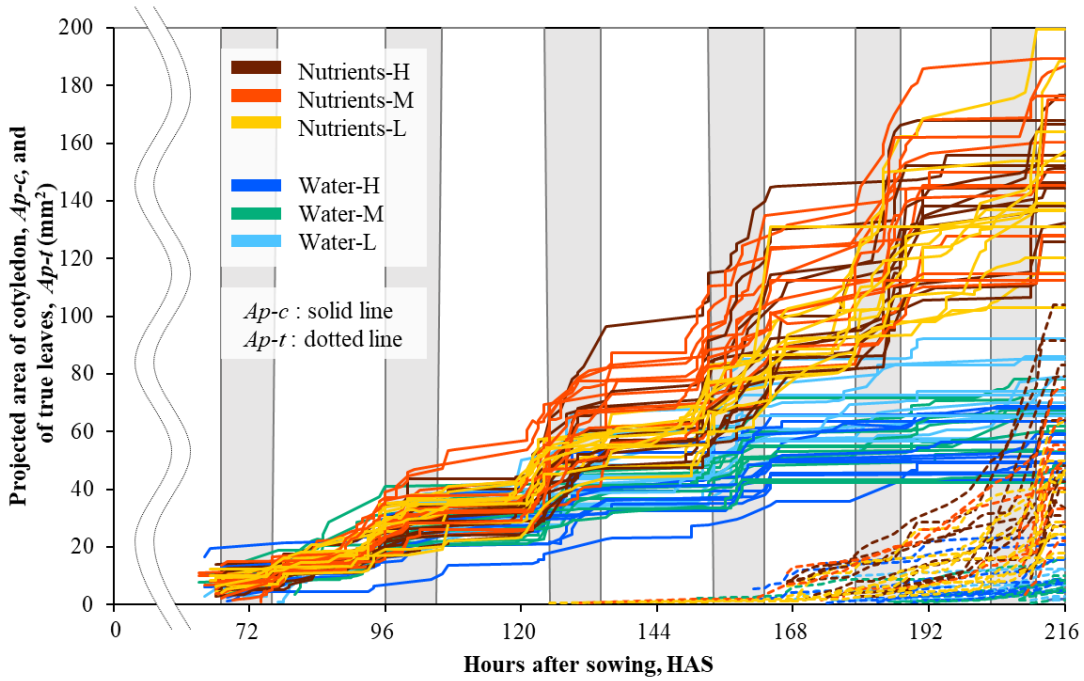

Figure 3-5. Time-course increasing changes in projected areas of the cotyledon (*Ap-c*) and true leaves (*Ap-t*) of individual seedlings with nutrients and water from hours to cotyledon unfolding from sowing (*Hc*) to 216 h after sowing (HAS), each with distributions of horizontal PPFDs (see Table 3-1 for treatments and codes).

Table 3-3 summarizes the average of *Hc* ($\overline{Hc}$), projected areas, including $\overline{Ap-c}$ both at cotyledon unfolding (*Hc*) and 216 HAS, and $\overline{Ap-t}$ and $\overline{Ap-ct}$ 216 HAS with nutrients and water, each with distributions of horizontal PPFDs (see Table 3-1 for treatments and codes). The slight difference in the initial $\overline{Ap-c}$ at cotyledon unfolding between the nutrients and water resulted in an approximately threefold difference in the $\overline{Ap-c}$ 216 HAS, along with $\overline{Ap-t}$, and thus, $\overline{Ap-ct}$ 216 HAS (Table 3-3). The $\overline{Ap-ct}$ with nutrients was more remarkable, in particular, caused by the growth of $\overline{Ap-t}$ (Table 3-3). As indicated in Table 3-3, $\overline{Ap-c}$, and especially $\overline{Ap-t}$ and $\overline{Ap-ct}$ 216 HAS, were larger with higher PPFD with nutrients.

Table 3-3. Average hours to cotyledon unfolding ($\overline{Hc}$), projected areas of cotyledon ($\overline{Ap-c}$) both at cotyledon unfolding and 216 h after sowing (HAS), true leaves ($\overline{Ap-t}$), and the sum of *Ap-c* and *Ap-t* ($\overline{Ap-ct}$), with nutrients and water, each with distributions of horizontal PPFDs (see Table 3-1 for treatments and codes).

Treatment Code	Hours to Cotyledon Unfolding ($\overline{Hc}$) [1]	Projected Cotyledon Area ($\overline{Ap-c}$) at *Hc* [2]	$\overline{Ap-c}$ 216 HAS	Projected Area of True Leaves ($\overline{Ap-t}$) 216 HAS	Projected Area of Cotyledon and True Leaves ($\overline{Ap-ct}$) 216 HAS
	h	mm²	mm²	mm²	mm²
Nutrients-H	67	10	138	54	192
Nutrients-M	65	8	138	43	172
Nutrients-L	66	8	124	36	157
Water-H	69	9	49	11	58
Water-M	66	8	55	7	62
Water-L	69	11	64	6	67

[1] Percentage of identified *Hc* of seedlings that could be estimated from the time series images was 56% with nutrients and 67% with water. [2] $\overline{Ap-c}$ at cotyledon unfolding.

Table 3-4 shows the average and coefficient of variation of the measured values 216 HAS, including areas of the cotyledon (*Ac*), true leaves (*At*) and the sum of individual *Ac* and *At* (*Act*), hypocotyl length (*Lh*), shoot fresh weight (*Wf*), shoot dry weight (*Wd*), and the ratio of *Act* to *Wd* (*LAR*) of individual seedlings with nutrients and water, each with distributions of horizontal PPFDs (see Table 3-1 for treatments and codes). The average *Ac* ($\overline{Ac}$), *At* ($\overline{At}$), and *Act* ($\overline{Act}$) values with nutrients were largest with Nutrients-H and the smallest with Nutrients-L. Furthermore, a greater coefficient of variation in *Ac*, *At*, and *Act* was shown with higher PPFD with nutrients, which was also demonstrated with *Wf*, *Wd*, and, to a lesser extent, with *LAR* (Table 3-4).

Table 3-4. Average and coefficient of variation of areas of the cotyledon (*Ac*), true leaves (*At*), and the sum of individual *Ac* and *At* (*Act*), hypocotyl length (*Lh*), shoot (cotyledon, true leaves, hypocotyl, and petiole) fresh weight (*Wf*), shoot dry weight (*Wd*), and the ratio of *Act* to *Wd* (*LAR*) of individual seedlings measured respectively 216 h after sowing (HAS) with nutrients and water, each with distributions of horizontal PPFDs (see Table 3-1 for treatments and codes).

	Treatment Code	**Area of Cotyledon (*Ac*)**	**Area of True Leaves (*At*)**	**Area of Cotyledon and True Leaves (*Act*)**	**Hypocotyl Length (*Lh*)**	**Shoot Fresh Weight (*Wf*)**	**Shoot Dry Weight (*Wd*)**	**The Ratio of *Act* to *Wd* (*Act*/*Wd*) (*LAR*)**
		mm^2	**mm^2**	**mm^2**	**mm**	**mg**	**mg**	**$m^2\ g^{-1}$**
Average	Nutrients-H	206	110	316	12	83.6	6.2	51
	Nutrients-M	205	102	307	13	84.0	6.0	52
	Nutrients-L	187	86	273	15	70.0	4.7	58
Coefficient of variation	Nutrients-H	0.131	0.258	0.157	0.139	0.206	0.208	0.096
	Nutrients-M	0.101	0.219	0.126	0.183	0.140	0.169	0.095
	Nutrients-L	0.101	0.123	0.090	0.137	0.058	0.095	0.081
Average	Water-H	71	14	84	10	24.5	3.3	26
	Water-M	72	15	88	10	25.2	2.9	30
	Water-L	82	13	96	12	26.9	2.7	36
Coefficient of variation	Water-H	0.155	0.315	0.138	0.147	0.167	0.195	0.222
	Water-M	0.260	0.675	0.210	0.148	0.164	0.205	0.156
	Water-L	0.159	0.385	0.187	0.112	0.209	0.208	0.150

Figure 3-6a shows the *Act* at 216 HAS and *Ap-ct* with nutrients and water. The value of *Ap-ct* varied depending on the timing due to the movement of the plants. The *Ap-ct* includes its values at 216 HAS and the maximum value over 216 h (MAX) (Figure 3-6a). The results showed that although the maximum *Ap-ct* over 216 h was slightly closer to the *Act*, the overall *Act* was greater than *Ap-ct*, notably with the nutrients (Figure 3-6a). Figure 3-2b shows the RGB image of the largest *Ap-ct* (with Nutrients-H) among 72 seedlings 216 HAS. In addition to the changes in the leaning of cotyledons and true leaves, slightly curled up cotyledon or true leaves decreased the value of *Ap-ct* (Figure 3-2b).

Figure 3-6b illustrates the ratio between *Ap-ct* and *Act* and *Wd* of individual seedlings at 216 HAS with nutrients and water. This implied that the ratio between *Ap-ct* and *Act* 216 HAS did not have an impact on the *Wd* of individual seedlings, but only suggested a significant difference in *Wd* affected by the difference in nutrients and water

(Figure 3-6b). The average ratio between *Ap-ct* and *Act* among individual seedlings with nutrients and water was 0.59 and 0.70, respectively, resulting in a greater average ratio of water to nutrients.

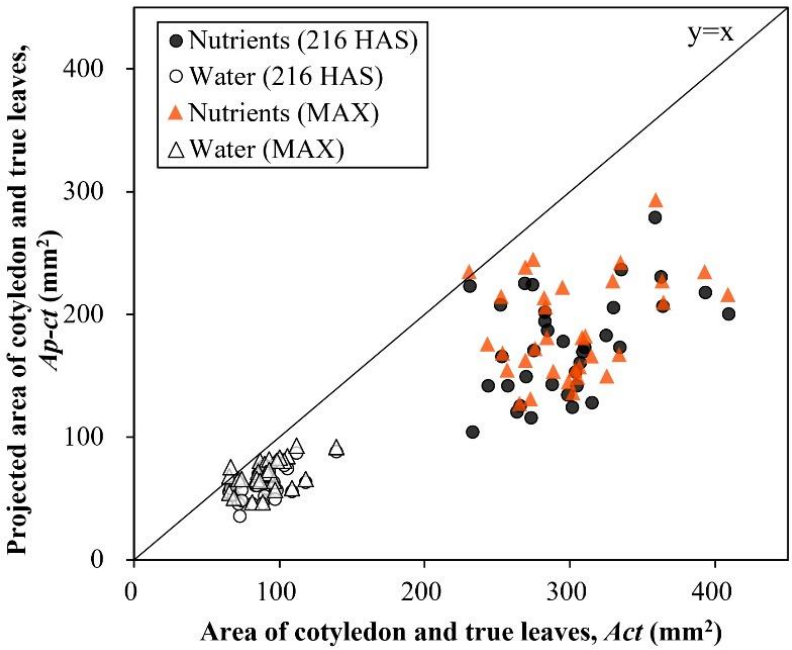

(**a**)

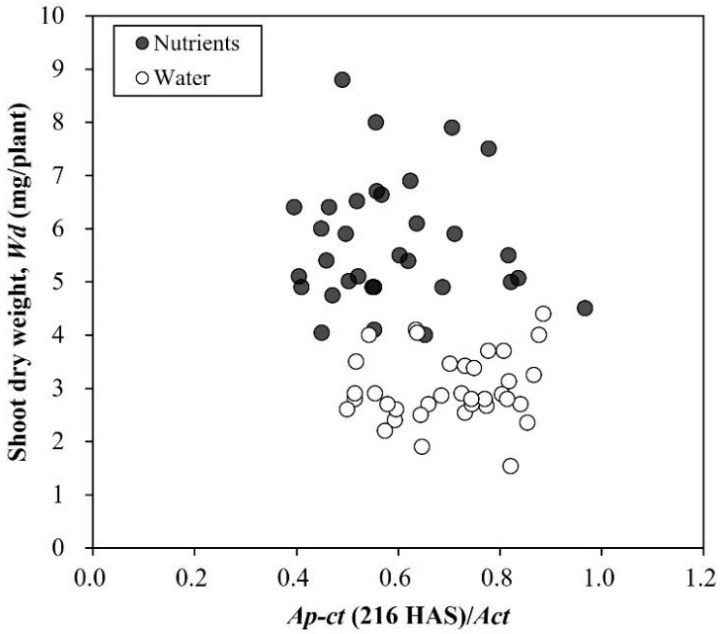

(**b**)

Figure 3-6. (a) The projected area of cotyledon and true leaves of the individual plants

(*Ap-ct*) and area of cotyledon and true leaves of individual plants 216 h after sowing (HAS) (*Act*), with nutrients and water. The *Ap-ct* includes its value at 216 HAS and the maximum value over 216 h. (b) The ratio between *Ap-ct* and *Act* (*Ap-ct*/*Act*) together with shoot (cotyledon, true leaves, hypocotyl, and petiole) dry weight (*Wd*) all at 216 HAS with nutrients and water.

Figure 3-7 illustrates the integrated PPFD from *Hc* to 216 HAS of each seedling and *Wd* with nutrients and water, each with distributions of horizontal PPFDs (see Table 3-1 for treatments and codes). Note that for some seedlings *Hc* could not be identified; those *Hc* were assumed to be $\overline{Hc}$ of 66.5 or 68 HAS with nutrients and water, respectively. This resulted in a greater *Wd* with nutrients, particularly with Nutrients-H, compared with water, as demonstrated in Figure 3-7. Furthermore, variations in *Wd* were found, especially with nutrients in the larger PPFD (Figure 3-7, Table 3-4). In fact, the coefficient of determination was small, both with nutrients and water (Figure 3-7).

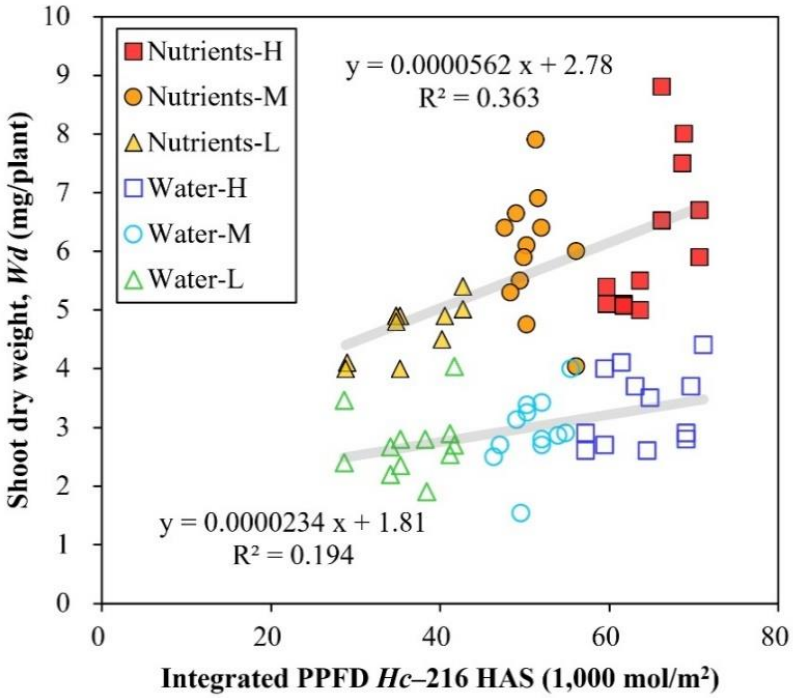

Figure 3-7. Integrated photosynthetic photon flux density (PPFD) from cotyledon unfolding (*Hc*) to 216 h after sowing (HAS) of each seedling and shoot (cotyledon, true

leaves, hypocotyl, and petiole) dry weight of individual seedlings 216 HAS (*Wd*), with nutrients and water, each with distributions of horizontal PPFDs (see Table 3-1 for treatments and codes).

3.4. Discussion

The objective of this study was to analyze the variations in the growth of cotyledons and initial true leaves, as affected by the surrounding microenvironment of varied PPFDs at individual seedlings and nutrients or water, based on the time series RGB image data captured every 0.5 h, along with individual measurements at 216 HAS.

For this study, seedlings, one of the critical initial stages of plant growth, were used as part of the plant cohort research with the MSPS, developed by improving a GCB equipped with a phenotyping unit and air temperature and relative humidity sensors [6]. The MSPS was designed with the high priority of installing cameras and sensors with low cost and compactness, emphasizing the practicality and scalability in commercial plant production and selection of seedlings for grading and breeding in PFALs.

In this study, the *Hc* of individual seedlings was estimated using the time course of the RGB images of individual seedlings. As *Hc* and *Wd* with nutrients and water demonstrated in Figure 3-3, the *Hc* of even the majority of seedlings varied at a maximum of 7 h, from 63–70 h. Although most cotyledon unfolding occurred in the dark period in this study, the difference in *Hc* may affect the integrated PPFD at each seedling in the case of the photoperiod.

With this individual analysis, a particular outlier of three seedlings with water with *Hc* of 77.5, 78.5, and 79 h, was found. One, with an *Hc* of 77.5 h, reached the second largest *Wd* (4.0 mg/plant) among the seedlings with water despite the unfavorable start, which implies the possibility of a delay in germination for some reason. The results demonstrated that $\overline{Hc}$ with nutrients was 1.8 h less than that with water (66.2 h with nutrients and 68 h with water). Moreover, variations in *Hc* with nutrients were smaller than those with water (Table 3-3). This indicates the possibility of promoting cotyledon unfolding by absorbing nutrients from radicles in addition to their heterotrophic nutrition

from the albumen of their seeds, which reflects the fact that all the *Hc* with nutrients occurred in the dark period. Furthermore, it can be presumed that seed phenotyping before sowing, including measuring the size, shape, or weight of seeds, enables the prediction of *Hc* or *Ac* at the cotyledon unfolding of the individual plant.

The results indicated that microenvironments, including varied PPFDs and nutrients or water, affected the phenotype or growth of individual seedlings (Figures 3-4–7, Tables 3-3, 3-4). The estimation of time series *Ap-c* and *Ap-t*, every 0.5 h based on the RGB images, revealed the relative individual changes over time, affected by varied PPFDs and the nutrients or water (Figures 3-4, 3-5, Table 3-3). Figures 3-4, 3-5 and Table 3-3 demonstrate that the initial *Ap-c* of 72 individuals varied over time in response to the surrounding microenvironment. With water, *Ap-c* remained comparatively constant even after the emergence of *Ap-t*, regardless of the PPFD (Figures 3-4, 3-5). In contrast, *Ap-c* with nutrients resulted in a continued relative increase throughout the experiment, even during the expansion of *Ap-t* (Figures 3-4, 3-5). With the nutrients, *Ap-ct* 216 HAS was the largest with Nutrients-H, and the smallest with Nutrients-L (Table 3-3).

Furthermore, Figure 3-4 demonstrates the time series movements of cotyledons and true leaves, including the changes in leaning or direction, in addition to the relative growth. As shown in Figure 3-4, each time-course *Ap-c* fluctuated more with the nutrients than with water. Indeed, the value of *Ap-ct* varies depending on the timing of the movement of plants. However, even with the maximum *Ap-ct* over 216 h, the result showed that the measured value, *Act*, was greater than *Ap-ct* 216 HAS, particularly with the nutrients (Figure 3-6a). Interestingly, the difference between *Ap-ct* and *Act* was caused by slightly curled up cotyledons or true leaves, and the changes in those leanings (Figure 3-2b). When comparing *Ap-ct* and *Act* at a specific moment, the ratio between *Ap-ct* and *Act* 216 HAS did not impact *Wd* of individual seedlings, but only suggested a significant difference in *Wd* affected by the difference in the nutrients and water (Figure 3-6b).

As shown in Figure 3-7 and Table 3-4, *Wd* was two-fold greater with nutrients than with water, resulting in a larger *Wd* with Nutrients-H. Although *Wd* was the largest with Nutrients-H and the smallest with Nutrients-L, it showed variations in *Wd*, especially with nutrients in the larger PPFD (Figure 3-7, Table 3-4). In this respect, the coefficient

of determination was small, both with the nutrients and water, i.e., 0.363 and 0.194, respectively (Figure 3-7). Furthermore, Table 3-4 shows a greater coefficient of variation in *Wd* with higher PPFD with nutrients (Nutrients-H 0.208, Nutrients-M 0.169, and Nutrients-L 0.095 for *Wd*), along with *Wf*, *Ac*, *At*, *Act,* and, to a lesser extent, *LAR*.

We acknowledge that this study has some limitations. First, a single RBG camera covered one tray to obtain the projected images; the viewing angle was not adjusted before estimating *Ap-c* or *Ap-t*. The growth variations were identified together with the actual measurements at 216 HAS (Figures 3-4, 3-5 and 3-7, Table 3-4). In future studies, the image capturing method can be improved in parallel with evaluating the light environment, which enables the estimation of time series leaf areas, leaf angles, and integrated photosynthetic photons received by individual leaves.

Second, there were limitations in estimating *Hc* based on RGB images. In practice, there were several obstacles in determining *Hc*, also in association with estimating *Ap-c* and *Ap-t*; seed coats remained attached to the cotyledon for some seedlings. Similar to the case of overlapping leaves, these issues will be resolved in future studies by improving the phenotyping system and applying automated determination of *Hc*, *Ap-c*, *Ap-t*, and *Ap-ct* by incorporating artificial intelligence (AI), along with analyzing the effects of additional microenvironment and management factors on the phenotype of individual plants.

In this study, by estimating *Hc* and time series *Ap-c*, *Ap-t*, and *Ap-ct*, in concurrence with the individual measurements of *Ac*, *At*, *Act, Wd*, and *Wf*, the variations in seedling growth were identified even under a similar microenvironment, including PPFD at individual seedlings and nutrients or water. Furthermore, the results demonstrated larger growth variations in the seedlings with higher relative growth with nutrients and larger PPFD. This may have been caused by the differences in seed lot with the same variety and genotypes, or by other microenvironmental effects, among other factors. In PFALs, where plant growth can be accelerated by environmental control, it is crucial to consider the effects of the microenvironment and uniformity of plant phenotype or growth. Based on the plant cohort research, selection of seedlings for grading and breeding along with plant production in PFALs may enable uniformity of plant phenotype

or growth and high productivity in commercial plant production, in view of simplified interactions of plant phenotypes with the microenvironment, management, and genotype for the life cycle of the plant.

3.5. Conclusions

In this study, experiments on the initial stage of seedlings, which strongly affect plant productivity, were conducted to analyze how the surrounding microenvironment of PPFDs and nutrients affects the variations in the growth of individual seedlings as part of research into the entire plant life cycle. A modular plant phenotype measurement system for seedling production was developed, which was designed with the high priority of installing cameras and sensors with low cost and compactness, emphasizing the system's practicality and scalability in commercial plant production in PFALs.

Using time series RGB images, cotyledon unfolding time and the time series projected area of cotyledons and true leaves of individual seedlings were obtained. In agreement with the actual individual measurements, variations in seedling growth were identified even under similar microenvironments. Furthermore, the results demonstrated larger variations in seedlings with higher relative growth.

With a view to simplifying interactions of plant phenotypes with the microenvironment, management, and genotype for the life cycle of the individual plant, selection of seedlings for grading and breeding, along with plant production in PFALs, may enable uniformity of plant phenotype or growth and higher productivity in PFALs.

Chapter 4. Variations in the seedling growth as affected by the time-course changes in photosynthetic photon flux density

4.1. Introduction

The uniformity of plant growth achieved by reducing two-dimensional (2D) variations in plant traits (i.e., phenotypes) can contribute to improving productivity in plant factories with artificial lighting (PFALs) [11,21]. Phenotypic variations in plant individuals are mainly attributable to three factors: environment, genotype (species and cultivar), and management (human and machine intervention, and seed treatments) [11,21]. The 2D variations in plant phenotypes over a cultivation tray are partially ascribed to 2D variations in the microenvironment surrounding individual plants, typically photosynthetic photon flux density (PPFD) and air current speed over and within the plant canopy or individuals in the tray, among other factors [21].

Previous studies have shown time-course changes in optimal PPFD or PPFD distribution over the cultivation tray depending on the stages of plant growth [23–26]. However, most previous studies were limited to simulations using software to examine the spatial distribution of PPFD in the cultivation space; thus, more studies with real plants are needed. Therefore, to elucidate how phenotypic variations are affected by the microenvironment of individual plants, it is critical to evaluate the time-course changes in PPFD over the cultivation tray and to study the effects of the time-course changes in the area percentage of plant leaves to the tray as the plant grows.

In this study, to examine the variations in seedling growth, owing to effects of the microenvironment, the effects of PPFD in the cultivation space, in particular time-course changes in PPFD even with constant photosynthetic photon flux (PPF) in response to the seedling growth, were investigated. First, initial experiments were conducted using artificial leaves as a replacement for plant leaves to examine the changes in PPFDs depending on the area percentage of the artificial leaves to either white substrate or black substrate tray (*APAL*), as affected by light reflection in the modular seedling production system (MSPS). Furthermore, to study the growth variations of seedlings as affected by the time-course changes in PPFD in response to seedling growth, experiments with real

seedlings were carried out for 14 days (336 h) from 11 days after sowing (DAS) to 25 DAS with white plug trays with white substrates.

4.2. Materials and Methods

4.2.1. Description of the System

An MSPS equipped with a phenotyping unit and an air temperature and relative humidity sensor was used, which was developed by modifying the germination container box (GCB) [6,11]. Figure 4-1 shows the configuration diagram of the MSPS used in this study. Two types of LEDs, an air circulator, and light-shielding sheet were additionally installed in the MSPS (L, O, M, and P; Figure 4-1) [6,11]. To maximize light reflection inside the MSPS, a reflection sheet was placed inside the exterior box (Q, Figure 4-1). However, no reflection sheets were placed above the LEDs.

The phenotyping unit, composed of red-green-blue (RGB) cameras and white LEDs for the flash, was activated every ten minutes (E and F; Figure 4-1) [6,11].

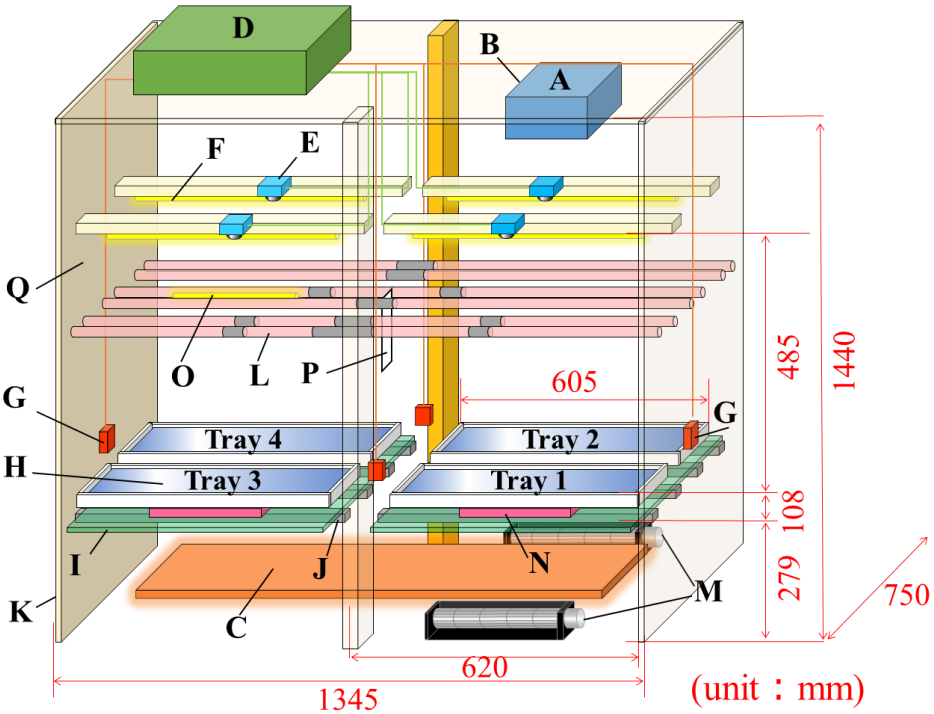

Figure 4-1. Modular seedling production system (MSPS) equipped with phenotyping unit and air temperature and relative humidity sensors [6,11]. LED (18 W each, length 1170 × width 30 × height 25 mm) (ZK-TB18-VE02/A; Fujian Sanan Sino-Science Photobiotech

Co., Ltd., Fujian, China) (×6) (L). Air circulator (DC12V 0.2A, blade size: 30 × 190 mm, length 240 × width 48 × height 50 mm) (a15110600ux0249jp; Uxcell, Hong Kong, China) (×2) (M). LED module (80Chip 12V, length 300 × width 6 × height 2 mm) (cob80-8420; Kaito Denshi Co., Ltd., Hasuda, Saitama, Japan) (O). Light-shielding sheet (length 200 × width 25 mm) (P). Reflection sheet (DNP Light Dispersion Film REFLEMO®; Dai Nippon Printing Co., Ltd., Shinjuku, Japan) (Q).

4.2.2. Light Environment for two settings

First, the light environment was regulated to maximize the uniformity of the horizontal photosynthetic photon flux density (PPFD) over the seedling trays by covering some parts of the six LEDs with aluminum tape (L, Figure 4-1). For each seedling tray (605 × 300 × 42 mm) with white substrates inside (white substrate tray), horizontal PPFDs, 0.04 m above the surface of the white tray at equally divided 18 sections per tray, were measured (× 4 trays) using PPFD sensors (accuracy ± 5 %) (LI-190R; LI-COR, Inc., Lincoln, NE, USA) with a data logger. The average horizontal PPFD over the white substrate tray was 213 ± 12.6 μmol m^{-2} s^{-1}.

To study the variations in seedling growth due to time-course changes in PPFD, a light environment over two trays (Trays 3 and 4) was designed to increase the PPF with a dimmable LED module, which was additionally installed above and between Trays 3 and 4 (O, Figure 4-1), in addition to six LEDs (L, Figure 4-1). With the additional dimmable LED, the PPF over Trays 3 and 4 was increased in response to the decrease in PPFD to maintain a constant initial value of PPFD (increased PPF). On the other hand, the remaining two trays (Trays 1 and 2) were set under constant PPF (fixed PPF), with only six LEDs (L, Figure 4-1).

The average ratio of the LED spectrum (L, Figure 4-1), blue: green: red: far-red, at the trays was 13:16:60:11 [11], whereas, the average spectrum of the additional dimmable LED (O, Figure 4-1), blue: green: red: far-red, was 40:39:19:2.

4.2.3. Experimental Design

4.2.3.1 Initial Experiments on the Changes in PPFD in response to the area percentage of leaves in the white and black trays

To examine the changes in PPFD according to the ratio of leaf area over the tray, initial two experiments were conducted using grass-green colored same-sized square pieces of papers (36.5 × 35.0 mm) (artificial leaves) as a replacement for plant leaves. Reflectance of the artificial leaves was 18%, as measured using an integrating sphere (diameter 125 mm, hole diameter 20 mm) (892032 JY959060; Jingyi optoelectronics Technology Co. Ltd., Jingyi, China) with white LED (ISL-150X150-series; CCS Inc., Kyoto, Japan). Reflectance values of white and black substrates (measured the same way) were 20 ± 7.8% and 0.9 ± 0.4%, respectively.

To study the changes in PPFD, with respect to light reflection inside the MSPS, two initial experiments were carried out with either white or black substrates filled inside the seedling trays (white substrate tray and black substrate tray, respectively). Artificial leaves with wire were horizontally placed 0.04 m above the white or black substrate tray (Tray 1), while for the remaining three white or black substrate trays (Trays 2, 3, and 4), artificial leaves were placed directly on the trays.

To measure PPFDs over both white and black substrate trays, five PPFD sensors were placed at the four corners and the center of the tray (Tray 1). During the measurement over white substrate trays, black-colored PPFD sensors, including black wires, were covered in white. PPFDs were measured 10 times with white substrate trays and seven times with black substrate trays, each with different area percentages of the artificial leaves, with respect to either white substrate or black substrate trays (*APAL*), from 0% (no artificial leaf) to 100% (full coverage with artificial leaves).

4.2.3.2. Experiments with Real Seedlings on the Time-course Changes in PPF and PPFD

Experiments with real seedlings were conducted for 14 days (336 h) from 11 DAS to 25 DAS to study the growth variations of seedlings, as affected by the time-course changes in PPFD in response to seedling growth.

A black plug seedling tray (589 × 300 ×45 mm, 128 cells) (Plug tray PP 128 holes; Ando Chemical Co., Ltd., Yamatokoriyama, Japan) was covered with white surface mulch (Kokage Mulch ® Delux; Okura Industrial Co. Ltd., Marugame, Japan) (white plug tray) to recreate a white tray. White substrates made of flexible polyurethane foam (584 × 280 × 29 mm, 300 cells, 23.3 × 23.3 × 29 mm per cell) (MIRAI Co., Ltd., Kashiwa, Japan) were used in the white plug trays. For the experiment with real seedlings, instead of a black substrate, a white substrate was used to maximize light reflection from the surface of the white plug trays inside the MSPS.

At 11 DAS, 62 out of 300 seedlings per white substrate tray, which were in relatively good condition and uniformly sized, were selected and transplanted into white plug trays at every other cell (62/tray × 4 = 248 seedlings). The remaining cells without seedlings were filled with white substrates. The PPFD sensors were placed at the center of each white substrate tray.

During the experimental period from 11 DAS to 25 DAS, PPF over Trays 3 and 4 was adjusted almost every day in incremental steps (from level 0 to 9) with dimmable LED to maintain a constant initial value of PPFD (increased PPF). In contrast, PPF was fixed throughout the experiment over Trays 1 and 2 (fixed PPF).

4.2.3.3. Plant Material and Culture Conditions

For experiments with real seedlings, coated seeds of romaine lettuce (*Lactuca sativa* L. var. longifolia, Lomaria, TLE487, Takii & Co., Kyoto, Japan) were used. Initially, for the preparatory cultivation of the experiments with real seedlings, 300 seedlings per white substrate tray (× 4 white substrate trays) were grown under the same settings with an average PPFD of 213 ± 12.6 μmol m^{-2} s^{-1} from 2 DAS until transplanting at 11 DAS. The volumetric percentage of the nutrient solution in the white tray was 86%

[6,11].

Throughout the experiment, the photoperiod was set at 16 h per day. For the nutrient solution, lettuce formula of Chiba University [59] was used, with pH and electrical conductivity of 6.5 and 0.2 S m^{-1}, respectively. At 11 DAS for transplanting, 2000 ml of nutrient solution was added to the white plug tray, and an additional 400 ml at 18 DAS and 500 ml at 22 DAS were added.

The average air temperatures inside the MSPS during the photoperiod and dark periods were 20 ± 0.5 °C and 20 ± 0.6 °C, respectively. The CO_2 concentrations during the photoperiod inside the MSPS were maintained at 1500 ± 50 μmol mol^{-1}. Air current speed 0.05 m above the surface of the trays was 0.16 ± 0.07 m s^{-1}, which was measured with a hot-wire anemometer (accuracy ± 2% or 0.02 m s^{-1}) (6531-21; KANOMAX JAPAN Inc., Suita, Osaka, Japan).

The MSPS was placed inside an environmentally controlled cultivation room for PFAL at the Kashiwanoha Campus of Chiba University. The air temperature, relative humidity, and CO_2 concentrations inside the cultivation room of PFAL were 20 °C, 80 ± 7%, and 1560 ± 168 μmol mol^{-1}, respectively.

4.2.3.4. Data Acquisition, variables, and symbols

As shown in Table 4-1, the average shoot fresh and dry weights ($\overline{Wf}$ and $\overline{Wd}$, respectively) were quantified at 25 DAS. $\overline{Wd}$ was measured after drying at 80 °C for 4 days in a thermostatic oven (accuracy ± 1 °C) (WFO-520W; TOKYO RIKAKIKAI Co., Ltd., Bunkyo-Ku, Tokyo, Japan). For weight measurement, a digital scale (linearity error ± 0.2 mg, precision 0.1 mg) was used after calibration.

To quantify $\overline{Wf}$ and $\overline{Wd}$, 62 plants were used for each treatment (Trays 3 and 4 for increased PF and Trays 1 and 2 for fixed PPF). To maximize the uniformity of each treatment with the two light environments, plants in the upper half (Tray 1 and 3) and the lower half (Tray 2 and 4) of each tray were measured for this study [31 plants/tray × 2 trays for each treatment (62 plants/treatment) × 2 treatments (124 plants)]. The remaining 124 plants, other than the 124 plants used for the measurement, were also cultivated together to replicate a light environment that could be affected by the density of the plant

canopy on a tray.

Table 4-1. List of symbols and variable names with descriptions and units.

Symbol	Variable name/Description	Unit
Fixed PPF	PPF remained constant in initial value	-
Increased PPF	PPF increased to maintain a constant initial value of PPFD	-
APAL	The area percentage of the grass-green colored same-sized square pieces of papers (artificial leaves) to the tray, with white substrates or black substrates	%
PPF	Photosynthetic photon flux	μmol s^{-1}
PPFD	Horizontal photosynthetic photon flux density 0.04 m above the surface of the tray	μmol m^{-2} s^{-1}
$\overline{Wd}$	Average shoot dry weight of 62 plants 25 days after sowing (DAS)	mg/plant
$\overline{Wf}$	Average shoot fresh weight of 62 plants 25 DAS	mg/plant

4.3. Results

In this study, to examine the variations in seedling growth, as affected by the time-course changes in PPFD in response to the area ratio of plant leaves to the tray, initial experiments were conducted using artificial leaves as a replacement for plant leaves to understand the changes in PPFDs with changing light reflection in the MSPS.

Figure 4-2 shows the changes in the PPFD in response to *APAL* with white and black substrate trays. Note that the reflectance of the artificial leaves was 18%. In the case of white substrate tray, where the initial average PPFD was 216 μmol m^{-2} s^{-1} with an *APAL* of 0% (no artificial leaves), PPFD gradually decreased to 179 μmol m^{-2} s^{-1} with an *APAL* of 100% (full coverage with artificial leaves), resulting in an overall 17% decrease in PPFD (Figure 4-2).

In contrast to the white substrate tray, the average PPFD over the black substrate tray resulted in 166 μmol m^{-2} s^{-1} with an *APAL* of 0% by just replacing white substrate tray with black substrate tray (Figure 4-2). As the *APAL* increased, PPFD over the black substrate tray slightly increased to 180 μmol m^{-2} s^{-1} with an *APAL* of 100% (full coverage with artificial leaves), resulting in an overall 8 % increase in PPFD (Figure 4-2).

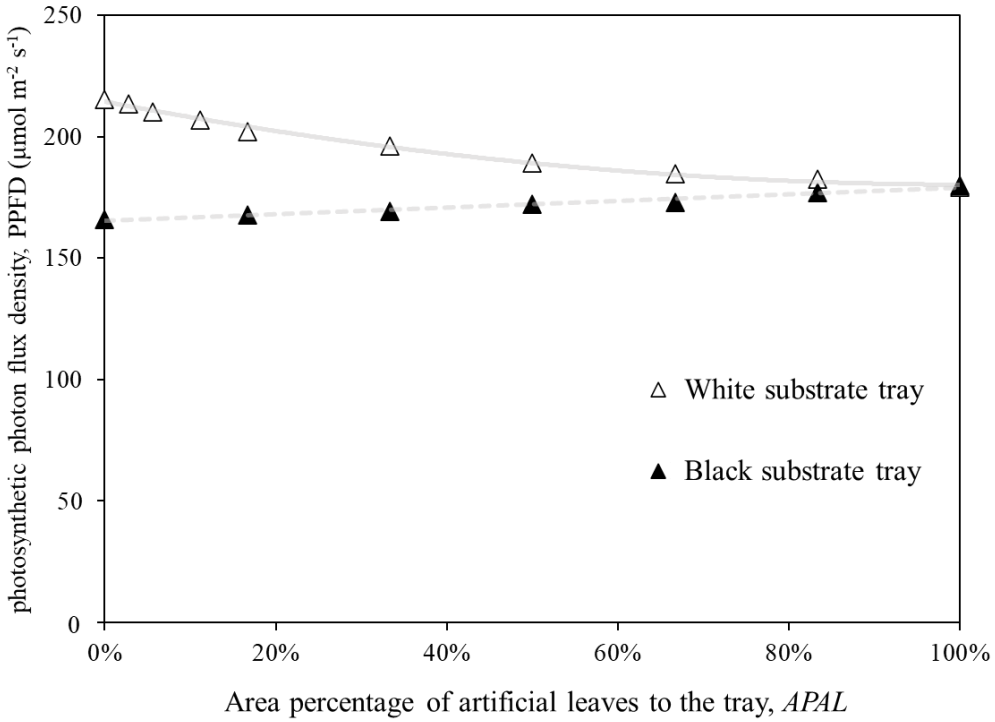

Figure 4-2. The changes in photosynthetic photon flux density (PPFD) in response to the area percentage of the grass-green colored same-sized square pieces of papers (artificial leaves) to the tray, with white substrates or black substrates. Reflectance of the artificial leaves was 18%.

To study the growth variations of seedlings with the time-course changes in PPFD in response to seedling growth, experiments with real seedlings were conducted for 14 days (336 h) from 11 DAS to 25 DAS. Figure 4-3 illustrates the time-course changes in PPFD in response to hours after transplanting (HAT) on white plug trays. Through the measurements of PPFD in total for 9 times at each white plug tray, PPF was increased gradually (from level 0 to 9), aiming at maintaining a constant initial value of PPFD (increased PPF). In contrast, PPF remained constant at the initial value without the control (fixed PPF). As shown in Figure 4-3, white plug trays with a fixed PPF resulted in a gradual decline in PPFD throughout the course of seedling growth. With a fixed PPF, while the initial value of PPFD started at 203 μmol m^{-2} s^{-1}, 0 HAT at 11 DAS, it appeared that the PPFD decreased to 149 μmol m^{-2} s^{-1} 312 HAT, with a total of 26% decrease in 13 days (Figure 4-3).

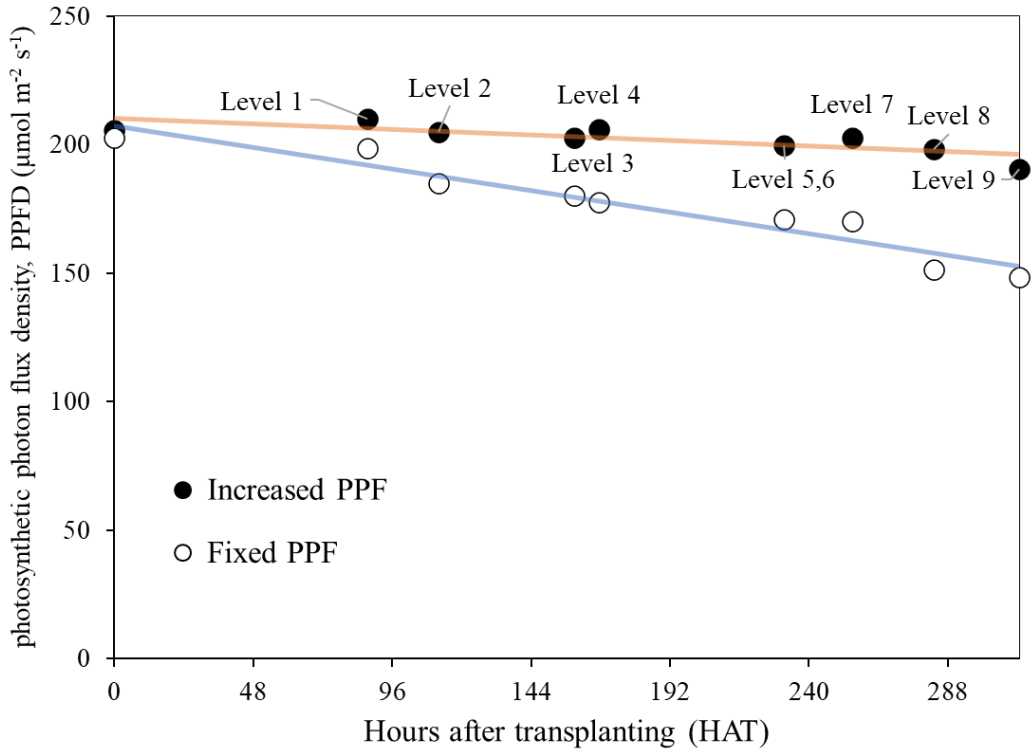

Figure 4-3. The time-course changes in photosynthetic photon flux density (PPFD) in response to hours after transplanting (HAT) on white plug trays with white substrates. Photosynthetic photon flux (PPF) was increased gradually (from level 0 to 9), aiming at maintaining a constant initial value of PPFD (increased PPF). On the other hand, PPF remained constant in initial value without control (fixed PPF).

Figure 4-4 illustrates $\overline{Wf}$ and $\overline{Wd}$ with fixed PPF and increased PPF (each treatment with 62 seedlings), which were measured at 25 DAS after 14 days of treatment. As demonstrated in Figure 4-4, both $\overline{Wf}$ and $\overline{Wd}$ appeared approximately 10% larger with the increased PPF than with fixed PPF. $\overline{Wd}$ with increased PPF and fixed PPF was 341 mg and 309 mg, respectively. Furthermore, $\overline{Wf}$ was 5,177 mg with increased PPF, whereas with fixed PPF, it was 4,743 mg.

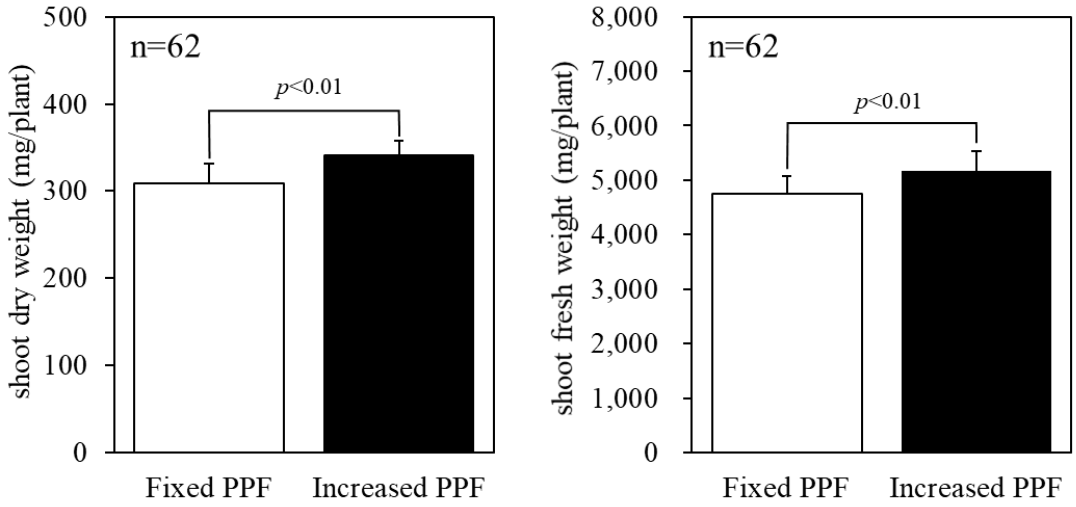

Figure 4-4. Average shoot dry weight and shoot fresh weight under fixed PPF and increased PPF; each treatment with 62 seedlings, measured 25 days after sowing.

4.4. Discussion

In this study, to examine the variations in seedling growth as affected by the microenvironment, the effects of PPFD in the cultivation space, in particular the time-course changes in PPFD even with fixed PPF in response to seedling growth, were studied. First, initial experiments were carried out using artificial leaves as a replacement for plant leaves to examine the changes in PPFDs depending on the *APAL*, as affected by light reflection in the modular seedling production system (MSPS). Furthermore, to study the growth variations of seedlings as affected by the time-course changes in PPFD in response to seedling growth, experiments with real seedlings were carried out for 14 days (336 h), from 11 DAS to 25 DAS, using white plug trays with white substrates.

The results indicated the changes in PPFD in response to *APAL* with white substrate tray; although the initial average PPFD was 216 μmol m^{-2} s^{-1} with an *APAL* of 0%, PPFD gradually decreased to 179 μmol m^{-2} s^{-1} with an *APAL* of 100%, resulting in a total of 17% decrease in PPFD. (Figure 4-3). This demonstrates that the PPFD decreased as the *APAL* increased. However, with the black substrate tray, the average PPFD remained relatively constant to the initial value of PPFD, which was 166 μmol m^{-2} s^{-1}

with an *APAL* of 0%. It is presumed that this difference in initial PPFDs between the white and black substrate trays was mainly due to white and black substrates having different reflectance values: 20 ± 7.8% and 0.9 ± 0.4%, respectively. With the black substrate tray, as the *APAL* increased, PPFD slightly increased to 180 μmol m^{-2} s^{-1} with an *APAL* of 100% and a total 8% increase in PPFD (Figure 4-2). It is estimated that this slight increase in PPFD over the black substrate tray was affected by the reflectance of artificial leaves, which had a reflectance of 18%.

As shown in Figure 4-3, with real seedlings cultivated on the white plug trays, the time-course PPFD with fixed PPF decreased as seedlings grew, starting with 203 μmol m^{-2} s^{-1} at 0 HAT and 11 DAS and reaching 149 μmol m^{-2} s^{-1} at 312 HAT, i.e., an overall 26% decrease in 13 days. In contrast, PPFD maintained an almost constant initial value during the experiment with increased PPF (Figure 4-3). These results indicate that the initial value of PPFD can decrease in response to plant growth or increasing value of area percentage of plant leaves in the cultivation tray, and thus, increasing PPF is needed to maintain a constant initial value of the desired PPFD level.

Furthermore, Figure 4-4 demonstrated that seedlings with increased PPF resulted in approximately 10% larger $\overline{Wf}$ and $\overline{Wd}$ than with the fixed PPF. This result indicates that by increasing PPF to maintain a constant initial value of PPFD, the relative growth of seedlings is greater than the decrease in PPFD when the PPF is not controlled.

This study has some limitations. First, PPFD with increased PPF could have been maintained more constantly at the initial value of PPFD by increasing PPF sufficiently. Second, there is a possibility that the light environment with fixed PPF was slightly affected by increasing PPF for the "increased PPF" condition. Without this effect, it is presumed that the PPFD with a fixed PPF was even lower than the result obtained in this experiment. These issues can be resolved by improving the experimental setup for enabling greater flexibility of, and controllability over the PPF. In future studies, PPF can be increased more profoundly, enabling the PPFD to increase as plants grow, which might cause more significant effects on plant growth than the constant PPFD. Furthermore, there is a limitation in applying artificial leaves to estimate *APAL* as a substitute for plant leaves. The time course of the projected leaf area (measured by 2D camera images captured from

above the plant canopy or seedling trays) of the plant canopy [11] can be applied using time series RGB images to quantify the area percentage of plant leaves to the cultivation tray in response to plant growth in future studies.

4.5. Conclusion

In this study, the effects of PPFD in the cultivation space, in particular the time-course changes in PPFD in response to seedling growth, were examined to determine the effects of the microenvironment on seedling growth. First, the use of artificial leaves as a replacement for plant leaves demonstrated changes in PPFDs depending on the *APAL*, as affected by light reflection in the MSPS with white and black substrates. Furthermore, the experiments with real seedlings carried out for 14 days (336 h) from 11 DAS to 25 DAS using white plug tray with white substrates, led to the growth variations of seedlings as affected by the time-course changes in PPFD in response to seedling growth. Additional studies with more profound and individual control of PPF in response to plant growth or time-course reduction in PPFD are needed to elucidate their effects on plant growth, as well as to enable the control of PPFD at its optimal value to improve plant productivity.

Acknowledgements

The author expresses her deep appreciation to Yumiko Amagai for her technical support for the system development and experiments.

Chapter 5. Conclusions

In this dissertation, research was conducted to identify variation in the plant phenotype or growth of individual plants and to analyze how phenotypic variations are affected by the surrounding microenvironment and management factors, using time series 2D images. PFALs with an almost airtight and well-insulated structure hold the potential to enable the production of large quantities of high-quality plants year-round while achieving high efficiency of resource utilization. However, despite the controlled environment in commercial PFALs, variations in plant individuals have been found, which has a negative impact on plant productivity in PFALs. Plant phenotyping plays a crucial role in understanding how the surrounding microenvironment of individual plants, management factors, and genotype affect variations in the time course of phenotypes of individual plants.

A modular plant phenotype measurement system for germination and seedling production was developed that focused on practicality and scalability in commercial PFALs, achieving a low cost with small cameras and sensors, and a cultivation method similar to commercial PFALs. Experiments on the germination and initial seedling stages of romaine lettuce (*Lactuca sativa* L. var. longifolia), which strongly affect plant productivity, were conducted as part of the plant life cycle research. In this dissertation, phenotypic analyses for germination time of individual seed and individual seedlings were conducted to identify the variations of individual plants affected by microenvironments, based on time series 2D images obtained every 0.5 h.

In this dissertation, using the developed plant phenotyping system, germination time of individual seeds was obtained and it revealed the variations in germination time affected by microenvironments of temperature and water volume and management factors of seed treatments in PFAL. Then, as a serial study, phenotypic analysis for seedlings, which was one of the further critical initial stages of plant growth, was conducted to analyze how the surrounding microenvironment of PPFDs and nutrients affect the variations in the growth of individual seedlings as part of the plant life cycle research. Cotyledon unfolding time and the time series projected area of cotyledons and true leaves of individual seedlings were obtained using time series RGB images. In agreement with

the respective actual measurements, variations in seedling growth were identified even under similar microenvironments. Furthermore, the results demonstrated more significant variations in seedlings with higher relative growth. Moreover, the effects of PPFD in the cultivation space, in particular the time-course changes in PPFD in response to seedling growth, were examined to determine the effects of the time-course microenvironment on seedling growth.

Through these studies, variations in plant phenotypes or growth were identified as affected by the surrounding microenvironment, including the surface temperature of individual seeds, PPFD and nutrients, and management factors such as seed processing (i.e., coated or uncoated seeds). Moreover, the time-course changes in PPFD over the cultivation space under the fixed PPF and its effects on the seedling growth were identified. In future studies, more experiments with additional microenvironment and management factors, considering the 2D or even 3D distribution over the plant cultivation trays, should be conducted, including subsequent plant growth stages as well to assess the impact of the variations in the whole plant growth process. These studies can be applied to more precise environmental control to improve the uniformity and productivity in PFALs.

With a view to simplified interactions of plant response with the microenvironment, management, and genotype for the life cycle of the individual plant history, in the future, selection of seedlings for grading and breeding along with plant production in PFALs could enable uniformity of plant phenotype or growth and higher productivity in PFALs.

References

1. Goto, E. Plant production in a closed plant factory with artificial lighting. *Acta Hortic*. **2012**, 956, 37–49. doi: 10.17660/ActaHortic.2012.956.2
2. Kozai, T. Resource use efficiency of closed plant production system with artificial light: concept, estimation and application to plant factory. *Proc Jpn Acad Ser B Phys Biol Sci*. **2013**, 89, 447–461. doi:10.2183/pjab.89.447
3. Leong, R.; Urano, D. Molecular Breeding for Plant Factory: Strategies and technology. In *Smart Plant Factory: The Next Generation Indoor Vertical Farms*; Kozai, T., Ed.; Springer: Berlin, 2018; 301–323.
4. Kozai, T.; Amagai, Y.; Hayashi, E. Towards sustainable plant factories with artificial lighting (PFALs): from greenhouses to vertical farms. In *Achieving sustainable greenhouse cultivation*; Marcelis, L., Heuvelink, E., Eds.; Burleigh Dodds Science Publishing: Cambridge, UK, 2019; 177–204.
5. Kozai, T.; Hayashi, E.; Amagai, Y. Plant factories with artificial lighting (PFALs) toward sustainable plant production. *Acta Hortic*. **2020**, 1273, 251–260. doi:10.17660/ActaHortic.2020.1273.34
6. Hayashi, E.; Amagai, Y.; Maruo, T.; Kozai, T. Phenotypic Analysis of Germination Time of Individual Seeds Affected by Microenvironment and Management Factors for Cohort Research in Plant Factory. *Agronomy* **2020**, 10, 1680, doi:10.3390/agronomy10111680.
7. Ohyama, K.; Yamaguchi, J.; Enjoji, A. Resource Utilization Efficiencies in a Closed System with Artificial Lighting during Continuous Lettuce Production. *Agronomy* **2020**, *10*, 723, doi:10.3390/agronomy10050723.
8. Orsini, F.; Pennisi, G.; Zulfiqar, F.; Gianquinto, G. Sustainable use of resources in plant factories with artificial lighting (PFALs). *Eur.J.Hortic.Sci.* **2020**, *85*, 297-309, doi:10.17660/eJHS.2020/85.5.1.
9. SharathKumar, M.; Heuvelink, E.; Marcelis, L.F. Vertical farming: moving from genetic to environmental modification. *Trends Plant Sci.* **2020**, *25*, 724-727, doi:10.1016/j.tplants.2020.05.012.
10. van Delden, S.; SharathKumar, M.; Butturini, M.; Graamans, L.; Heuvelink, E.; Kacira, M.; Kaiser, E.; Klamer, R.; Klerkx, L.; Kootstra, G. Current status and future challenges in implementing and upscaling vertical farming systems. *Nat Food* **2021**, *2*, 944–956, doi:10.1038/s43016-021-00402-w.
11. Hayashi, E.; Amagai, Y.; Kozai, T.; Maruo, T.; Tsukagoshi, S.; Nakano, A.; Johkan, M. Variations in the Growth of Cotyledons and Initial True Leaves as Affected by Photosynthetic Photon Flux Density at Individual Seedlings and Nutrients. *Agronomy* **2022**, 12, 194, https://doi.org/10.3390/agronomy12010194
12. Hayashi, E. Selected PFALs in Japan. In *Plant Factory*: *An indoor vertical farming system for efficient quality food production* 2nd Edition; Kozai, T., Niu, G. and Takagaki, M. Eds.; Academic Press, 2019; 437-454.
13. Kozai, T. PFAL business and R&D in Asia and North America: status and perspectives. In *Plant Factory*: *An indoor vertical farming system for efficient quality food production* 2nd Edition; Kozai, T., Niu, G. and Takagaki, M. Eds.; Academic Press, 2019; 35-39.
14. Takakura, T., Kozai, T., Tachibana, K., Jordan, K.A. Direct digital control of plant growth - I. Design and operation of the system. Trans. ASAE **1974**, 17 (6), 1150e1154.
15. Takatsuji, M. Plant Factory with Artificial Lighting (written in Japanese: Shokubutsu Kojo). Koudan-sha (Blue backs), 1979; p. 232.
16. Hayashi, E. Current Status of Commercial Plant Factories with LED Lighting Market in Asia, Europe, and Other Regions. In *LED lighting for urban agriculture*; Kozai, T., Fujiwara, K. and Runkle, E. Eds.; Springer: 2016; 295–308.

17. Japan Greenhouse Horticulture Association
18. Kozai, T. Benefits, problems and challenges of plant factories with artificial lighting (PFALs): a short review. In Proceedings of the International Symposium on New Technologies for Environment Control, Energy-Saving and Crop Production in Greenhouse and Plant 1227, 2017; pp. 25-30, doi:10.17660/ActaHortic.2018.1227.3.
19. Kozai, T., Uraisami, K., Kai, T., Hayashi, E. Indexes, definition, equation and comments on productivity of plant factory with artificial lighting (in Japanese). *Nogyo oyobi Engei* **2019**, *94*, 661-672.
20. Kozai, T.; Uraisami, K.; Kai, K.; Hayashi, E. Productivity: definition and application. In *Plant Factory Basics, Applications and Advances*, Kozai, T., Niu, G., Masabni, J., Eds.; Elsevier: Amsterdam, Netherlands, 2022; pp. 197-216, doi:10.1016/B978-0-323-85152-7.00009-4.
21. Kozai, T.; Lu, N.; Hasegawa, R.; Nunomura, O.; Nozaki, T.; Amagai, Y.; Hayashi, E. Plant Cohort Research and Its Application. In *Smart Plant Factory: The next generation indoor vertical farms*, Kozai, T., Ed.Kozai, T., Ed.; Springer: Berlin, Germany, 2018; pp. 413-431, doi:10.1007/978-981-13-1065-2_26.
22. Nagano, S.; Moriyuki, S.; Wakamori, K.; Mineno, H.; Fukuda, H. Leaf-movement-based growth prediction model using optical flow analysis and machine learning in plant factory. *Front. Plant Sci.* **2019**, *10*, 227, doi:10.3389/fpls.2019.00227.
23. Goto, E.; Takakura, T. Relationship between Light Intensity and Light Energy Requirementin the Growth of Leaf Vegetables under Artificial Light (in Japanese). *J Agr.Met* **1987**, 43, 229-232.
24. Akiyama, T.; Kozai, T. Light Environment in the Cultivation Space of Plant Factory with LEDs. In *LED Lighting for Urban Agriculture*, Kozai, T., Fujiwara, K., Runkle, E., Eds.; Springer Nature: Singapore, 2016; pp. 91-109, doi:10.1007/978-981-10-1848-0_7.
25. Kim, J.; Kang, W.H.; Son, J.E. Interpretation and evaluation of electrical lighting in plant factories with ray-tracing simulation and 3D plant modeling. *Agronomy* **2020**, *10*, 1545, doi:10.3390/agronomy10101545.
26. Saito, K.; Ishigami, Y.; Goto, E. Evaluation of the Light Environment of a Plant Factory with Artificial Light by Using an Optical Simulation. *Agronomy* **2020**, *10*, 1663, doi:10.3390/agronomy10111663.
27. Soltani, E.; Ghaderi-Far, F.; Baskin, C.C.; Baskin, J.M. Problems with using mean germination time to calculate rate of seed germination. *Aust. J. Bot.* 2015, 63. doi: 10.1071/BT15133
28. Kitajima, K. Impact of cotyledon and leaf removal on seedling survival in three tree species with contrasting cotyledon functions1. *Biotropica* 2003, *35*, 429-434, doi:10.1111/j.1744-7429.2003.tb00597.x.
29. Hanley, M.E.; May, O.C. Cotyledon damage at the seedling stage affects growth and flowering potential in mature plants. *New Phytologist* **2006**, *169*, 243-250, doi:10.1111/j.1469-8137.2005.01578.x.
30. Zhang, H.; Zhou, D.; Matthew, C.; Wang, P.; Zheng, W. Photosynthetic contribution of cotyledons to early seedling development in Cynoglossum divaricatum and Amaranthus retroflexus. *N.Z. J. Bot.* **2008**, *46*, 39-48, doi:10.1080/00288250809509752.
31. Zheng, W.; Wang, P.; Zhang, H.; Zhou, D. Photosynthetic Characteristics of the Cotyledon and First True Leaf of Castor (*Ricinus communis* L.). *Aust. J. Crop. Sci.* **2011**, *5*, 702-708, doi:10.3316/informit.282042581359260.
32. Kumar, J.; Pratap, A.; Kumar, S. Phenomics in Crop Plants: Trends, Options and Limitations. Springer: New Delh, India, 2015.
33. Fiorani, F.; Schurr, U. Future Scenarios for Plant Phenotyping. Annual Review of Plant Biology 2013, 64:1, 267–291.

34. Golbach, F.; Kootstra, G.; Damjanovic, S.; Otten, G.; Van de Zedde, R. Validation of plant part measurements using a 3D reconstruction method suitable for high-throughput seedling phenotyping. *Machine Vision and Applications* **2016**, 27, 663–680.
35. Ninomiya, S.; Baret, F.; Cheng, Z.-M. Plant phenomics: emerging transdisciplinary science. *Plant Phenomics* 2019. https://doi.org/10.34133/2019/2765120
36. Guo, W.; Zheng, B.; Duan, T.; Fukatsu, T.; Chapman, S.; Ninomiya, S. EasyPCC: Benchmark Datasets and Tools for High-Throughput Measurement of the Plant Canopy Coverage Ratio under Field Conditions. *Sensors* **2017**, 17, 798. https://doi.org/10.3390/s17040798.
37. Feldman, A.; Wang, H.; Fukano, Y.; Kato, Y.; Ninomiya, S.; Guo, W. EasyDCP: An affordable, high-throughput tool to measure plant phenotypic traits in 3D. *Methods Ecol. Evol.* **2021**, 1679-1686, doi:10.1111/2041-210X.13645.
38. Guo, W. Automated Characterization of Plant Growth and Flowering Dynamics Using RGB images. In Smart Plant Factory: The Next Generation Indoor Vertical Farms; Kozai, T., Ed.; Springer: Berlin, 2018; 385–393.
39. Shibata, T.; Iwao, K.; Takano, T. Growth prediction of lettuce plants by image processing. In Proceedings of the International Symposium on Transplant Production Systems 319, **1992**; pp. 689-694, doi:10.17660/ActaHortic.1992.319.111.
40. Giacomelli, GA.; Ling, P.P.; Morden, RE. An automated plant monitoring system using machine vision. *Acta Hort.* **1996**, *440*, 377-382, doi: 10.17660/ActaHortic.1996.440.66.
41. Itoh, H.; Yamamoto, H. A Modeling of Lettuce Growth by System Identification (Part 1) (in Japanese). *Journal of the Japanese Society of Agricultural Machinery* **2005**, *67*, 6, 71-80.
42. Franchetti, B.; Ntouskos, V.; Giuliani, P.; Herman, T.; Barnes, L.; Pirri, F. Vision based modeling of plants phenotyping in vertical farming under artificial lighting. *Sensors* **2019**, *19*, 4378, doi:10.3390/s19204378.
43. Jayalath, T.C.; van Iersel, M.W. Canopy Size and Light Use Efficiency Explain Growth Differences between Lettuce and Mizuna in Vertical Farms. *Plants* **2021**, *10*, 704, doi:10.3390/plants10040704.
44. Tian, Z.; Ma, W.; Yang, Q.; Duan, F. Application status and challenges of machine vision in plant factory—A review. *Information Processing in Agriculture* **2021**, doi:10.1016/j.inpa.2021.06.003.
45. Furuyama, S.; Ishigami, Y.; Hikosaka, S.; Goto, E. Estimation of Lighting Energy Consumption Required for Red Leaf Lettuce Production under Different Blue/Red Ratios and Light Intensity Conditions in a Plant Factory with Artificial Lighting (in Japanese). *Shokubutsu Kankyo Kogaku*, **2017**, 29, 60-67.
46. Kozai, T., Ed. *Smart Plant Factory: The Next Generation Indoor Vertical Farms*. Springer: Berlin, 2018.
47. Hayashi, E.; Kozai, T. Phenotyping and AI-based Environmental Control and Breeding for PFAL. In *Smart Plant Factory: the next generation indoor vertical farms*; Kozai, T., Ed.; Springer: Berlin, 2018; 405–411.
48. Kuijken, R.C.; van Eeuwijk, F.A.; Marcelis, L.F.; Bouwmeester, H.J. Root phenotyping: from component trait in the lab to breeding. *J Exp Bot*. **2015**, 66, 5389–5401. doi:10.1093/jxb/erv239
49. Bewley, J.D.; Bradford, K.J.; Hilhorst, H.W.M.; Nonogaki, H. *Seeds: physiology of development, germination and dormancy*, 3rd ed.; Springer: New York, USA, 2013.
50. Baskin, C.C.; Baskin, J.M. *Seeds: ecology, biogeography, and evolution of dormancy and germination*, 2nd ed.; Elsevier/Academic Press: San Diego, USA, 2014.
51. Gustin, J.L.; Settles, A.M. Seed Phenomics. In *Phenomics: How Next-Generation Phenotyping is Revolutionizing Plant Breeding*; Fritsche-Neto. R., Borém, A., Eds.; Springer: Switzerland, 2015; 67–82.

52. Ducournau, S.; Feutry, A.; Plainchault, P.; Revollon, P.; Vigouroux, B.; Wagner, M.H. Using computer vision to monitor germination time course of sunflower (*Helianthus annuus* L.) seeds. *Seed Sci. & Technol*. **2005**, 33, 329–340.
53. Shinohara, T. Seed Vigour as a New Seed Quality lndex and lts Utility. *Japanese Society of Agricultural Technology Management* **2009**, 16, 1–9 (in Japanese).
54. Joosen, R.V.; Kodde, J.; Willems, L.A.; Ligterink, W.; van der Plas, L.H.; Hilhorst, H.W. GERMINATOR: a software package for high-throughput scoring and curve fitting of Arabidopsis seed germination. *Plant J*. **2010**, Apr 1;62(1), 148-59.
55. Ligterink, W., Hilhorst, H.W.M. High-Throughput Scoring of Seed Germination. In *Plant Hormones*; Kleine-Vehn, J., Sauer, M., Eds.; Methods in Molecular Biology, vol 1497. Humana Press, New York, NY. 2017. https://doi.org/10.1007/978-1-4939-6469-7_7
56. Hasegawa, R. Data warehouse for plant phenotyping in plant factories. Proceedings of the meeting of Japanese Society of Agricultural, Biological and Environmental Engineers and Scientists (JSABEES). Tokyo, 2018; 224–225.
57. R Core Team. R: A Language and Environment for Statistical Computing; R Foundation for Statistical Computing: Vienna, Austria, 2019.
58. International Seed Testing Association (ISTA). International Rules for Seed Testing. Zurich: International Seed Testing Association. 2019.
59. Maruo, T.; Ito, T.; Ishii, S. Studies on the feasible management of nutrient solution in hydroponically growth lettuce (Lactuca sativa L.). *Tech. Bull. Fac. Hort. Chiba Univ*. **1992**, 46, 235–240.
60. Kikuzawa, K. The basis for variation in leaf longevity of plants. *Vegetatio* **1995**, *121*, 89-100, doi:10.1007/BF00044675.
61. Santos, H.P.; Buckeridge, M.S. The role of the storage carbon of cotyledons in the establishment of seedlings of Hymenaea courbaril under different light conditions. *Ann. Bot.* **2004**, *94*, 819-830, doi:10.1093/aob/mch209.
62. Walter, A.; Scharr, H.; Gilmer, F.; Zierer, R.; Nagel, K.A.; Ernst, M.; Wiese, A.; Virnich, O.; Christ, M.M.; Uhlig, B. Dynamics of seedling growth acclimation towards altered light conditions can be quantified via GROWSCREEN: a setup and procedure designed for rapid optical phenotyping of different plant species. *New Phytol*. **2007**, 174, 447-455, doi:10.1111/j.1469-8137.2007.02002.x.
63. Darwin, C.; Darwin, F. *The power of movement in plants*; John Murray: 1880.
64. Hoshi, T.; Takiguchi, T. Continuous Measurement of Movement in Spinach Leaves Using Video Cameras (in Japanese). *Journal of Agricultural Meteorology* **1995**, *51*, 123-130, doi:10.2480/agrmet.51.123.
65. Schneider, C.A.; Rasband, W.S.; Eliceiri, K.W. NIH Image to ImageJ: 25 years of image analysis. *Nat. Methods.* **2012**, *9*, 671-675, doi:10.1038/nmeth.2089.